Available online at www.sciencedirect.com
SCIENCE DIRECT
Journal of Asian Earth Sciences 28 (2006) 185–204
Journal of Asian Earth Sciences
www.elsevier.com/locate/jaes

Protolith of eclogites in the north Qaidam and Altun UHP terrane, NW China: Earlier oceanic crust?

Jingsui Yang [a,*], Cailai Wu [a], Jianxin Zhang [a], Rendeng Shi [a], Fancong Meng [a], Joseph Wooden [b], Houng-Yi Yang [c]

[a] *Key Laboratory for Continental Dynamics of MLR Institute of Geology, Chinese Academy of Geological Science, 262 Baiwanzhuang Road, Beijing 100037, China*
[b] *Department of Geological and Environmental Sciences, Stanford University, Stanford, CA 94305, USA*
[c] *Department of Earth Sciences, National Cheng Kung University, Tainan, Taiwan, China*

Received 5 May 2004; received in revised form 14 December 2004; accepted 14 September 2005

Abstract

An early Paleozoic ultrahigh pressure metamorphic belt occurs in the north Qaidam–Altun mountains and was offset about 400 km southwestward by the Altyn Tagh strike-slip fault. Eclogites in the belt consist of major basaltic and minor picritic rock types and can be subdivided into three groups: high TiO_2 (2–5 wt%), medium TiO_2 (1–2 wt%) and low TiO_2 (<1 wt%). Geochemical evidence shows that the protoliths of the eclogite were basaltic rocks from different tectonic environments, including mid-ocean ridge basalt, island arc basalt and ocean island basalt. The Nd isotopes of these rocks are similar to those of MORB, characterized by mainly positive and minor negative εNd(0) values, providing further evidence that the eclogite protoliths were ocean floor basalts to which minor crustal components were added during subduction. Geochronological data indicate that the UHPM occurred about 500–440 Ma ago, and that there were two eclogite protoliths with ages of 800–750 and ~1000 Ma, respectively. Geochemically and isotopically, the eclogites are similar to basaltic rocks in Luliangshan, north Qaidam mountains, which have Sr and Nd ages of 768±39 and 780±22 Ma. The age and composition of these volcanic rocks suggest that they were one type of the protoliths for the eclogites. A later series of calc-alkaline, island arc volcanic rocks was formed at about 500 Ma ago, essentially contemporaneous with the UHP metamorphism.

We propose the following tectonic model for the evolution of the north Qaidam UHP belt. At about 1000 Ma ago, a number of continents were amalgamated to form the Rodinian continent in this general area, which contained some oceanic volcanic rocks, possibly as ophiolitic fragments. This part of Rodinia was then rifted at about 800–750 Ma ago to form an oceanic basin with a variety of MORB and ocean island basalts. Closure of this ocean basin produced the Neoproterozoic ophiolites and granitic gneisses in the north Qaidam mountains. In the early Paleozoic another Qilian ocean basin formed and subduction of this oceanic lithosphere formed the island arc volcanic rocks at about 500 Ma ago and the subduction-related granites (470–450 Ma). Once the oceanic lithosphere was consumed, the subsequent continent–continent collision led to deep subduction of continental crust, which was tectonically mixed with the eclogites, to cause the ultrahigh pressure metamorphism.

Keywords: UHPM; Eclogite; Qilian; North Qaidam; Altun

1. Introduction

Most eclogites in ultrahigh-pressure metamorphic (UHPM) belts have basaltic protoliths that were derived from the subducted plate, and hence record the processes of plate subduction/collision and exhumation. A 350 km-long eclogite belt of Paleozoic age was recently recognized in the north Qaidam mountains (Yang et al., 1998, 2000; Zhang et al., 2000), which is located in the west part of the Central Orogenic Belt in China. Coesite inclusions in zircon from some of the gneissic country rocks (Yang et al., 2001a, 2002b), as well as pseudomorphs of coesite and exsolution structures in some UHP minerals in the eclogite (Song and Yang, 2001), provide critical evidence for UHP metamorphism and deep subduction of continental crust. The north Qaidam UHPM belt is believed to connect westward to the Altun eclogite belt, which has been offset about 400 km by the Altyn Tagh strike-slip (Xu et al., 1999; Yang et al., 2001b). U–Pb and Ar–Ar dating of

* Corresponding author. Tel.: +86 10 6899 7804; fax: +86 10 6899 4782.
E-mail address: yangjsui@ccsd.cn (J. Yang).

1367-9120/$ - see front matter © 2006 Elsevier Ltd. All rights reserved.
doi:10.1016/j.jseaes.2005.09.020

the eclogite and its gneissic country rock indicate an early Paleozoic age for the UHP metamorphism, with eclogite in the north Qaidam mountains being dated at 495 ± 6 Ma, and that in Altun at 500 ± 10 Ma (U–Pb TIMS, Zhang et al., 2000, 2002). Associated with the UHP rocks are subduction-related I- and S-type granites, as well as a suite of early Paleozoic island arc volcanic rocks whose age is similar to that of the UHP metamorphism and granites (Wu et al., 2002; Li et al., 1999; Shi et al., 2004a). However, the genetic relationship between the UHPM rocks, granites and island arc volcanic rocks, if any, is still unclear. Was there subduction of oceanic crust before the continental subduction, which was responsible for the formation of the volcanic rocks and granites?

This paper reports geochemical, geochronological and Nd isotopic data for the eclogites of this belt, their protoliths and some related basaltic rocks in the north Qaidam mountains. These data are then used to discuss the tectonic setting of the continental collision and deep subduction.

2. Occurrences of north Qaidam and Altun Eclogites and Luliangshan Basaltic rocks

The northern margin of the Tibetan Plateau consists of a giant mountain range thousands of kilometer long and hundreds of kilometer wide. From west to east, this belt includes the West Kunlun mountains, the Altun mountains and the Qilian mountains. The Qilian mountains extend for about 800 km in a WNW direction, are over 300 km wide, and consist of the Qilian micro-continental block bounded by the north Qilian Suture (NQLS) and north Qaidam Suture (NQDS). The NQLS, which separates the Qilian micro-continental block from the Alxa block to the north (Fig. 1), contains numerous ophiolites and high pressure (HP) blueschists and eclogites of early Paleozoic age (Xiao et al., 1978; Wu et al., 1993; Xu et al., 1994; Shi et al., 2004b). The NQDS separates the Qilian micro-continent from the Qaidam–East Kunlun micro-continent to the south, and contains the UHP eclogites, island arc volcanic rocks and granites discussed in this paper (Yang et al., 2000).

The eclogites in the NQDS occur as tectonic blocks or layers and constitute a 2 to 5-km-wide belt within the gneissic rocks of the Dakendaban Group of Neoproterozoic age (Fig. 2A–D). The Dakendaban Group is a suite of middle- to high-grade gneiss, schist and marble, and is covered by the Quanji Group of Neoproterozoic age, composed of less deformed and metamorphosed sandstone, conglomerate and limestone (Geological Bureau of Qinghai Province, 1991; Yang et al., 1998). The zicon from the early Paleozoic island arc volcanic rocks, which are characterized by greenschist facies metamorphism, yielded a U–Pb age of 514 ± 8 Ma (Shi et al., 2004a). SHRIMP U–Pb dating of the zircons from the associated I- and S-type granites yielded ages of 473 ± 15 and 446 ± 10 Ma, respectively (Wu et al., 2002).

Lower Paleozoic strata in the north Qaidam mountains are composed of middle-Cambrian, Ordovician and Silurian sequences, which are overlain by the upper Paleozoic strata of Devonian and Carboniferous ages. A major conglomerate with large and unsorted clasts occurs at the base of the Devonian sequence. The conglomerates contain both granitic and basaltic clasts, which range up to 1 m in diameter and are mostly well-rounded. The upper part of the Devonian sequence is dominated by continental detrital rocks and some intermediate-felsic volcanic rocks. The lower part of the Carboniferous sequence is coarse-grained sandstone unconformably overlying the Ordovician and Devonian strata. Upper Carboniferous strata consist of biogenic limestone, suggesting formation

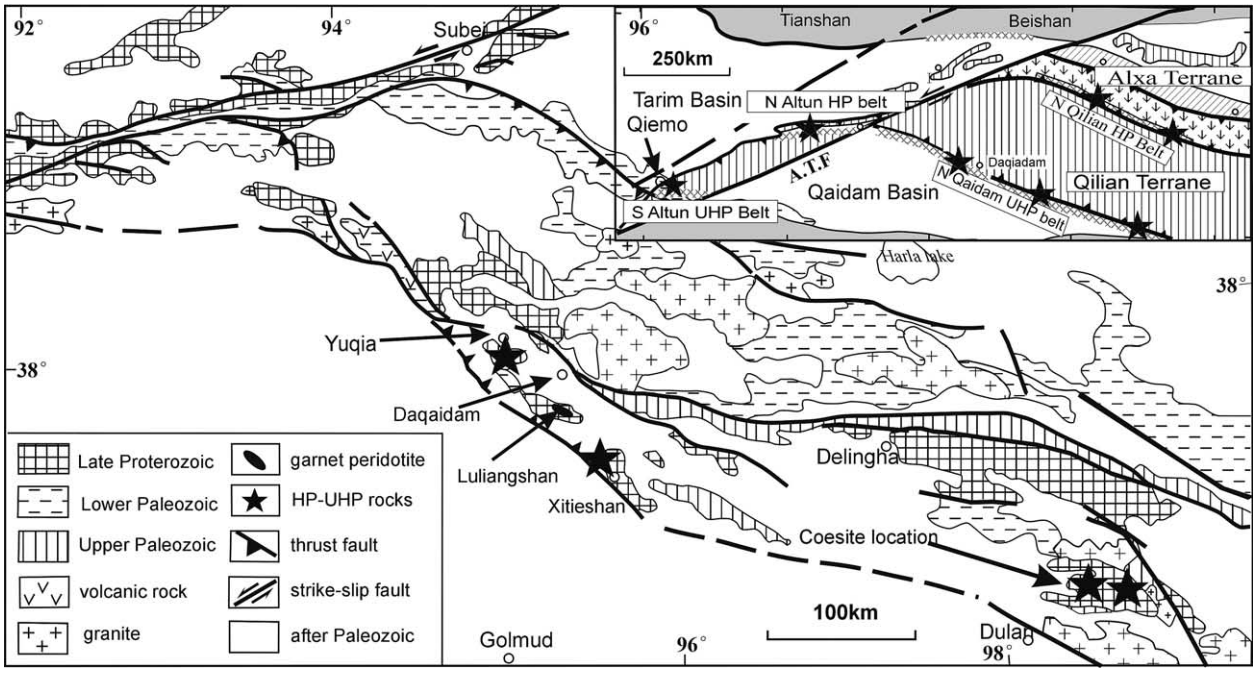

Fig. 1. A simplified geological map of the north Qaidam–South Altun region, showing the main localities of the eclogite.

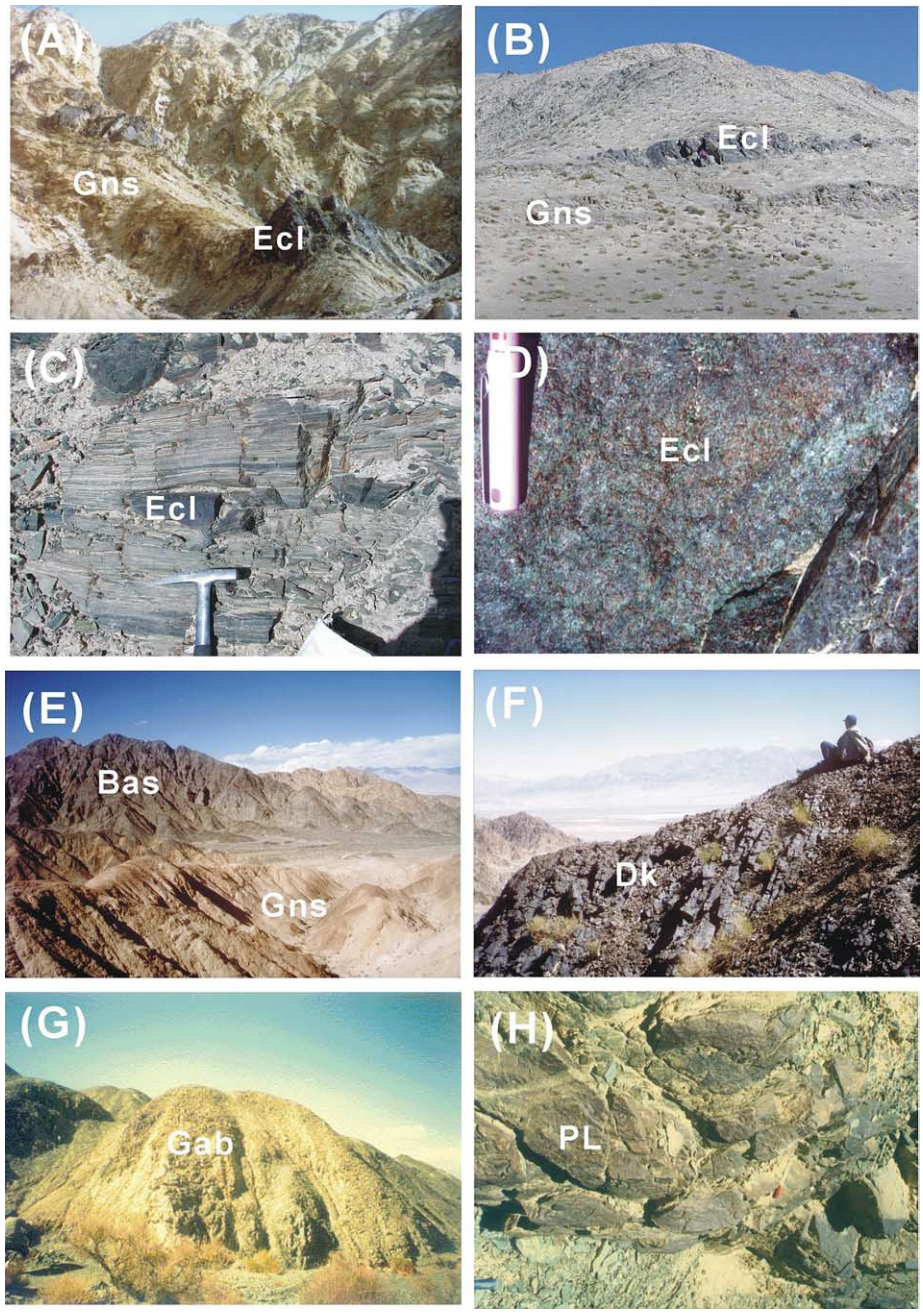

Fig. 2. Occurrences of the eclogites and basaltic rocks in the north Qaidam mountains. (A) Eclogite (Ecl) lens in gneiss (Gns), Daqaidam; (B) eclogite interlayers in gneiss, NBD; (C) eclogite retrograded to amphibolite and gneiss, NBD; (D) fresh outcrop of eclogite, NBD; (E) Basaltic rocks (Bas) associated with gneiss in Luliangshan, north Qaidam; (F) diabase dikes, (Dk) Luliangshan; (G) gabbros (Gab), Luliangshan; (H) Pillow lavas (PL), Luliangshan.

in a shallow marine environment. Sparse Jurassic and Cretaceous strata are also present in the region. The former consists of coal-bearing lake-swamp deposits, whereas the latter are mainly composed of lacustrine deposits (Geological Bureau of Qinghai Province, 1991).

Eclogite mainly occurs in the Daqaidam, Xitieshan and Dulan regions (Fig. 1). Eclogite was first reported in Daqaidam where it occurs as pods in the garnet–muscovite gneiss of the Dakendaban Group. Over 50 pods have been found in this region in a belt about 3 km wide and over 10 km long. Eclogites in Xitieshan, which were discovered in 1999, are mostly retrograded so that only a very few fresh pods have been located. In Dulan the eclogite forms numerous pods in Proterozoic strata of the Shaliuhe Group, which can be correlated with the Dakendaban Group. The pods crop out in a belt about 10 km wide but are of unknown length.

Eclogite in the Altun mountains has been mainly observed in the Qiemo region, where it occurs as lenticular bodies in garnet-bearing gneiss, felsic gneiss, plagioclase amphibole gneiss, and sillimanite-bearing, K-feldspar gneiss. Generally, the eclogite is highly retrograded so that from the center to the margin of a block, it is progressively replaced by garnet

amphibole gneiss. The country rock in which the eclogite occurs is characterized by a high amphibolite to granulite facies mineral assemblage, but to date no UHPM minerals have been found in these rocks.

Most blocks of eclogite are less than 20×10 m, but some are measured up to 100×50 m, with their long directions parallel to the foliation of the gneiss; some eclogites occur as layers within the gneiss. Five distinct belts of eclogite are recognized, designated as the Daqaidam Eclogite Belt, the Xitieshan Eclogite Belt, the northern Dulan Eclogite Belt, the Southern Dulan Eclogite Belt, and the Altun Eclogite Belt, respectively, in this paper.

In addition, some mafic and ultramafic rocks occur in a zone hundreds of meters wide in the north Qaidam mountains, particular in the Luliangshan region, south of Daqaidam, and in this paper these rocks are called as the Luliangshan basaltic sequence. These rocks are in tectonic contact with the gneiss and are mainly volcanic rocks with some sheeted dikes and gabbros. Pillow lavas have been identified in these rocks and some ultramafic blocks were also observed in the field (Fig. 2E–H). All of them have been metamorphosed to the amphibolite facies rocks. Geochemical characteristics of the Luliangshan basaltic rocks, including some diabase dikes and gabbros, have been discussed and compared with those of eclogites in different belts in following sections.

3. Mineralogy of the eclogites

3.1. The Eclogite in the Daqaidam belt

In general, most eclogites in Daqaidam are fresh and characterized by the assemblage garnet+omphacite+phengite+rutile. Microprobe analysis shows that the garnets consist mainly of almandine (alm) (44–62 mol%), grossular (gr) (15–33 mol%) and pyrope (pyr) (12–30 mol%) and that they plot in groups C and B of Coleman (1965) (Fig. 3A). The omphacites consist of 37–46 mol% jadeite (Jd) and 50–57 mol% augite (Aug) and that they plot within the omphacite field (Omp) (Fig. 3B). The Si content of phengite varies from 6.6 to 6.9 atoms/formula unit, whereas Mg ranges from 0.6 to 0.8 and Fe from 0.21 to 0.25 atoms/formula unit based on a stoichiometry of 22 oxygen atoms. Peak metamorphic conditions are calculated as T=680–730 °C and P=2.3–2.8 GPa (Yang et al., 1998; Zhang et al., 2002).

3.2. Eclogite in the Xitieshan Belt

All of the eclogites in Xitieshan have been extensively retrograded and fresh material occurs only in the central parts of some garnet amphibolite blocks. Peak metamorphic minerals are garnet+omphacite+rutile; no phengite has been observed in these rocks. The cores of garnet have 47–50 mol% pyrope, 28–31 mol% almandine and 17–22 mol% grossular (Fig. 3A), richer in pyrope than those in other eclogites in the region. Omphacite has a smaller jadite component (22–26 mol%) (Fig. 3B). The peak metamorphism of eclogite took place at T=770–830 °C and P>1.4 GPa, but exsolution of quartz needles in omphacite suggests that the rocks underwent UHP metamorphism (Zhang et al., 1999; Carswell et al., 1997; Tsai and Liou, 2000).

3.3. The Eclogite in the Southern Dulan belt (SDB)

In the SBD, the peak metamorphic minerals in eclogite are garnet+omphacite+rutile+kyanite, and no phengite has been observed. These garnets consist mainly of almandine (38–54 mol%), with lesser grossular (21–24 mol%) and pyrope (19–37 mol%) (Fig. 3A). The omphacite contains 3–4 wt% Na_2O and has 24–38 mol% jadeite (Fig. 3B), which is lower than the omphacite in Daqaidam (37–46 mol%) (Yang et al., 1998). Kyanite is common in the eclogite of this belt, but has not been observed in either the Daqaidam or northern Dulan belts. However, kyanite is common in eclogites of the Dabie-Sulu UHP metamorphic belt (Wang et al., 1992), where the peak metamorphic pressure is estimated to be over 2.7–2.9 GPa. Garnet–omphacite co-existing pair suggests that metamorphism took place at T=856–896 °C and $P \geqq$1.6–1.8 GPa (Yang et al., 2000).

3.4. The Eclogite in the northern Dulan belt (NBD)

The peak metamorphic mineral assemblage in the northern Dulan eclogite is: garnet+omphacite+phengite(Si 6.9)+rutile. Kyanite has not been found in these rocks, although it is common

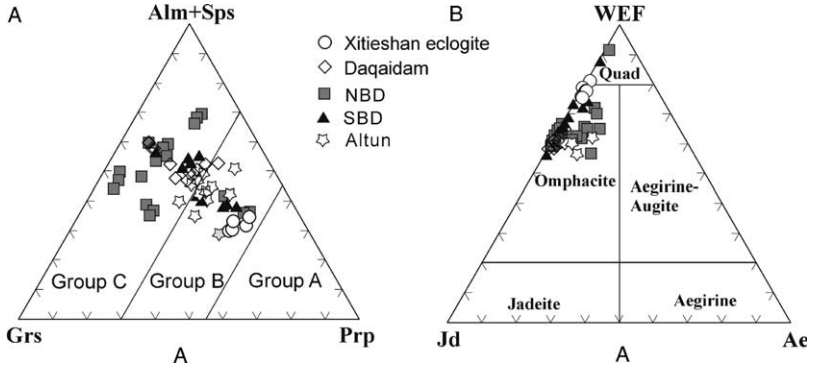

Fig. 3. (A) Garnets from eclogites in the north Qaidam–Altun UHPM terrane are plotted in the regions of group C and group B eclogites (Coleman et al., 1965); (B) jadeite molecules of the clinopyroxene.

Table 1
Chemical compositions of the eclogite from the north Qaidam and Altun Mountains

Location Sample num	1 Daqaidam 31-34	2 Daqaidam 31-35a	3 Daqaidam 32-8.	4 Daqaidam 32-12.	5 Daqaidam 32-56	6 Daqaidam DY-K-8	7 Daqaidam ZM-6-9.1	8 Xitieshan XT-37	9 Xitieshan XT-38	10 Xitieshan XT-46	11 Xitieshan XT-49	12 Xitieshan XT-51	13 Xitieshan XT-58-1	14 Xitieshan Z-J01-10-1	15 NBD 99Y-102	16 NBD 99Y-113	17 NBD 99Y-115	18 NBD 99Y-308-B	19 NBD 99Y-313	20 NBD 99Y-318	21 NBD 99Y-319	22 SBD 99Y-72	23 SBD 99Y-201-2	24 SBD 99Y-205	25 SBD 99Y-207	26 SBD 99Y-221	27 Altun 97A-12-1	28 Altun 96A-14-5	29 Altun 97A-12	30 Altun 97A-12-Q	31 Altun 97A-12-2	32 Altun AJ-9
SiO_2	45.98	46.42	45.85	46.13	49.48	50.92	47.77	48.97	49.86	47.65	45.08	46.66	49.83	49.8	46.34	42.52	46.39	49.39	47.52	48.35	47.63	48.74	44.61	47.95	42.94	42.66	49.72	49.56	49.40	51.28	51.24	51.80
TiO_2	3.43	3.37	2.39	1.83	0.94	0.58	0.69	0.44	1.13	1.17	1.12	0.54	1.18	1.09	1.66	5.48	1.66	1.15	2.16	1.78	1.97	0.18	0.77	0.58	0.74	0.78	1.75	1.51	1.71	1.20	1.41	1.34
Al_2O_3	15.31	16.05	15.32	15.32	14.59	14.25	14.85	11.31	14.83	15.46	16.52	14.99	14.7	15.46	10.88	12.88	11.33	12.8	13.94	11.96	11.16	21.77	20.57	14.63	18.65	18.35	14.33	12.91	13.96	13.73	13.78	13.13
Fe_2O_3	4.45	3.48	2.98	3.3	0.75	1.3	3	1.27	1.39	1.07	1.79	1.73	2	1.85	5.28	4.31	5.52	3.22	2.93	3.38	3.74	0.72	3.68	3.47	4.05	4.13	4.02	2.35	3.49	2.04	2.04	1.74
FeO	9.93	10.15	10.15	9.86	11.64	6.9	10.04	7.42	10.88	12.22	10.15	7.45	9.47	8.12	10.64	17.7	10.70	9.58	13.08	11.96	12.46	3.38	10.92	8.23	10.47	12.37	8.89	9.79	9.32	9.14	10.40	9.25
MnO	0.2	0.2	0.21	0.22	0.23	0.16	0.22	0.19	0.22	0.23	0.21	0.17	0.2	0.17	0.26	0.31	0.26	0.2	0.15	0.23	0.26	0.079	0.17	0.23	0.23	0.26	0.21	0.20	0.21	0.19	0.21	0.19
MgO	6.3	6.21	7.06	7.27	6.66	9.51	8.23	13.89	7.43	7.79	9.45	13.21	7.72	7.96	7.75	5.49	7.76	8.69	7.91	6.63	6.32	7.53	5.04	9.57	7.23	6.03	7.53	7.55	7.17	7.62	6.89	8.77
CaO	10.22	9.23	11.32	11.21	11.69	12.35	13.42	14.03	11.05	11.25	12.7	11.96	11.43	11.51	13.15	9.05	12.64	12.48	9.29	11.71	12.21	12.13	10.94	12.22	12.49	11.28	11.06	11.98	10.99	11.09	11.23	11.07
Na_2O	3.15	3.01	2.41	1.7	2.18	2.69	0.74	0.94	2.12	1.92	1.52	1.11	1.8	2.06	2.59	1.16	2.91	1.71	2.13	2.66	2.66	2.85	1.99	2.12	1.39	1.46	2.18	1.93	2.20	2.33	1.92	1.84
K_2O	0.5	1.25	0.67	0.57	0.02	0.09	0.14	0.27	0.39	<0.1	<0.1	0.25	0.16	0.24	0.20	0.49	0.22	0.09	0.21	0.33	0.32	0.29	0.21	0.31	0.15	0.63	0.16	0.02	0.19	0.44	0.01	0.43
P_2O_5	0.4	0.44	0.28	0.13	0.09	0.06	0.06	<0.05	0.12	0.07	0.07	0.05	0.1	0.1	0.10	0.10	0.10	0.10	0.17	0.20	0.10	0.10	0.20	0.10	0.10	0.10						0.11
LOI	1.11	1.13	1.45	1.99	1.3			0.62	<0.1	0.12	0.37	1.08	0.32		0.60	<0.05	0.08	0.30	0.10	0.48	0.44	2.22	0.76	0.48	0.68	1.18						0.1
H_2O^+						0.2	0.46							0.6																		
CO_2						0.63	0.18							0.46																		
Total	100.98	100.94	100.09	99.53	99.57	98.81	99.16	99.35	99.42	98.95	98.98	99.20	98.91	98.36	99.45	99.49	99.57	99.71	99.59	99.67	99.27	99.99	99.86	99.89	99.12	99.23	100.10	99.25	99.28	99.60	99.40	99.77
La	24.5	23.49	17.43	7.51	1.35	0.83	1.43	1.28	4.43	1.78	6.42	1.04	5.55	6.22	1.86	33.9	5.72	3.8	16.1	9.75	12.6	1.36	5.48	7.4	6.39	6.2	7.01	2.09	10.40	4.70	5.03	8.74
Ce	47.38	46.49	34.27	15.27	2.68	1.72	2.41	3.52	11.44	4.54	16.06	3.05	14.7	14.6	3.47	72.7	13.8	47.12	31.4	23	27.2	2.77	11.3	15.9	16.3	11.4	15.12	4.40	21.65	10.50	12.54	20.06
Pr	5.9	5.8	4.14	2.07	0.53	0.23	0.56	0.5	1.52	0.57	1.97	0.42	1.81	1.96	0.45	8.32	1.98	1.06	3.65	2.4	3.06	0.38	1.67	2.2	1.69	1.21	2.06	0.78	2.31	1.57	1.13	2.35
Nd	26.04	24.88	18.42	9.66	3.07	1.1	3.25	2.57	7.11	3.15	10.54	2.44	9.17	9.12	2.05	38.4	9.04	5.28	19.7	11.4	14.8	1.72	8	9.84	10.6	5.8	9.50	3.25	12.77	6.74	8.40	11.27
Sm	6.59	6.33	4.82	3.01	1.38	0.45	1.44	1.03	2.34	1.48	2.9	0.86	3.02	2.58	0.97	8.81	2.52	1.82	5.36	3.43	4.21	0.49	2.02	2.27	2.86	1.37	3.62	2.00	4.12	2.83	3.07	3.16
Eu	2.36	2.28	1.64	1.2	0.59	0.17	0.64	0.34	0.79	0.68	1.01	0.39	0.83	1	0.51	2.59	0.94	0.73	1.79	1.26	1.34	0.33	0.94	0.8	0.88	0.68	1.50	1.11	1.61	1.21	1.27	1.03
Gd	6.24	6.64	5.23	4.05	3.69	1.22	2.62	1.13	2.56	2.67	2.83	1.14	2.83	3.26	2.36	9.66	3.54	2.61	7.43	5.04	5.2	0.75	2.39	2.83	3.06	1.7	4.61	3.68	4.98	4.05	3.86	3.29
Tb	0.91	0.94	0.67	0.79	0.64	0.37	0.56	0.23	0.49	0.56	0.49	0.22	0.54	0.6	0.48	1.52	0.61	0.49	1.1	0.8	1	0.11	0.31	0.35	0.46	0.21	0.75	0.65	0.75	0.60	0.70	0.59
Dy	4.93	4.68	4	5.39	4.62	3.07	3.93	1.46	3.13	3.48	3.12	1.21	3.23	3.85	3.1	9.35	3.58	2.94	6.25	4.92	5.7	0.56	1.68	1.94	2.59	1.16	5.02	4.47	4.87	3.83	4.59	3.80
Ho	1.02	1	0.88	1.14	1.16	0.76	0.86	0.31	0.69	0.73	0.72	0.42	0.67	0.84	0.76	1.78	0.93	0.74	1.04	1.26	0.83	0.14	0.41	0.48	0.64	0.29	0.89	0.86	0.92	0.72	0.86	0.74
Er	2.73	2.57	2.23	3.07	3.47	2.35	2.66	0.9	1.99	1.95	1.92	0.9	1.76	2.46	1.38	4.91	1.72	1.36	3.93	2.35	4.06	0.26	0.74	0.88	1.2	0.51	2.46	3.37	2.46	2.02	2.28	1.87
Tm	0.32	0.31	0.28	0.47	0.5	0.36	0.4	0.12	0.28	0.29	0.26	0.16	0.26	0.35	0.23	0.6	0.28	0.23	0.45	0.39	0.45	0.038	0.11	0.15	0.19	0.084	0.35	0.35	0.36	0.28	0.33	0.29
Yb	1.85	1.87	1.64	2.8	3.21	2.38	2.7	0.71	1.72	1.82	1.54	0.88	1.48	2.25	1.44	3.31	1.83	1.46	2.57	2.52	2.77	0.25	0.69	0.95	1.18	0.53	2.34	2.22	2.26	1.80	2.13	1.59
Lu	0.28	0.28	0.25	0.44	0.5	0.36	0.41	0.13	0.28	0.3	0.23	0.13	0.25	0.34	0.21	0.5	0.28	0.22	0.34	0.38	0.41	0.037	0.1	0.15	0.18	0.08	0.38	0.32	0.34	0.26	0.28	0.22
Y	24.01	23.8	20.24	29.99	30.05	17.8	22.8	9.62	24.63	25.25	25.16	11.54	25.07	19	12.7	41.4	15.4	12.6	29.1	22.5	29.1	2.37	6.72	7.88	10.6	4.4	26.17	23.31	25.22	19.17	23.19	21.68
Sc	15.21	15.66	19.81	27.6	34.61	52.5	48.9	53.51	46.63	48.66	41.99	36.67	42.33	43.7	19.2	23	26.9	24.8	24.6	29	27.7	12.5	24.5	27.6	32.1	27.4	25.84	30.75	25.58	22.76	25.50	35.31
Rb	16	29	32	34	0.76	3.69	1.99	10	5.9	7	7.5	22	19	8.59	6.02	26	4.99	2.54	6.62	3.98	9.36	19.2	8.25	11.7	6.89	17.5	11.00		14.00	23.00		23
Sr	330	246	292	150	41	30.7	84.9	70.16	74.42	85	72.42	69.56	88.52	151	59	158	38.4	64.1	69.1	257	167	270	766	447	687	496	157.50		166.20	139.70		104.6
Ba	171	393	168	162	6.58	132	16.2	36.53	33.07	9.32	13.02	33.59	25.93	46.8	219	292	225	185	199	250	249	196	231	236	228	318	27.16		35.12	71.43		92.88
Zr	121	128	89	71	15	37	36.9	21	68	53	43	25	41	77	27.3	254	13.7	5.8	47.5	138	31	21.9	26.9	20	25.2	16.9	62.00		63.00	30.00		86
Nb	23	24	17	11	3	2.56	0.73	1	3.9	2.8	1.7	1.1	2.6	5.74	4.6	19.9	1.45	0.88	3.78	4.84	10.8	0.32	0.25	0.53	0.49	0.23	8.00		9.00	6.00		2.3

(*continued on next page*)

Table 1 (*continued*)

Location	1	2	3	4	5	6	7	8	9	10	11	12	13	14	15	16	17	18	19	20	21	22	23	24	25	26	27	28	29	30	31	32
Sample	Daq-aida-m	Daq-aida-m	Daq-aida-m	Daq-aida-m	Daq-aida-m	Daq-aida-m	Daq-aida-m	Xiti-esh-an	Xiti-esh-an	Xiti-esh-an	Xiti-esh-an	Xiti-esh-an	Xiti-esh-an	Xiti-esh-an	NBD-99Y-102	NBD-99Y-113	NBD-99Y-115	NBD-99Y-308-B	NBD-99Y-313	NBD-99Y-318	NBD-99Y-319	SBD-99Y-72	SBD-99Y-201-2	SBD-99Y-205	SBD-99Y-207	SBD-99Y-221	Alt-un	Alt-un	Alt-un	Alt-un	Alt-un
num	31-34	31-35a	32-8.	32-12.	32-56	DY-K-8	ZM-6-9.1	XT-37	XT-38	XT-46	XT-49	XT-51	XT-58-1	J01-10-1													97A-12-1	96A-14-5	97A-12	97A-12-Q	97A-12-2	AJ-9
Ta	0.9	0.64	0.43	0.32	0.71	0.16	0.18	0.2	0.8	0.6	0.4	0.7	0.3	0.52	0.19	0.56	0.087	0.05	0.2	0.008	0.44	0.025	0.092	0.065	0.034	0.019						0.3
U	0.62	1.5	0.32	0.82	0.16	0.08	0.07	0.3	0.5	0.2	0.4	<0.1	0.3	0.21	0.093	0.44	0.14	0.11	0.38	0.18	0.27	0.059	0.16	0.25	0.14	0.15						0.8
Th	2.73	2.78	1.38	1.24	0.32	0.34	0.03	0.3	0.9	3.3	0.7	<0.1	0.6	1.35	0.029	3.36	0.75	0.26	2.28	0.89	1.29	0.034	0.12	0.16	0.14	0.09						2.5
Hf	1.59	0.99	0.47	0.52	0.9	1.3	1.65	0.8	2.4	2.1	1.6	0.9	1.6	2.3	0.46	0.87	0.52	0.17	0.81	4.11	0.59	0.33	0.52	0.36	0.46	0.37						2.8
V	239	213	199	199	203	215	274	222.4	311.4	328.1	294.8	165.1	304.5	275	463	547	537	434	362	441	547	129	453	402	601	585						268.9
Cr	74	73	96	105	112	470	216	621	227	345	402	1010	353	283	161	151	218	414	231	148	132	365	33	345	79.5	55.1						506
Ni	76	66	62	57	100	134	95.7	252	102	94	213	299	139	97.8	88.4	46.1	101	120	81.9	27	70.8	127	4.2	65.4	25	5.35						149
Co	47	43	45	35	52	49.3	37.8	54.97	50.66	40.31	46.13	43.76	39.64	48.9	58.1	50.1	55.2	49.9	55.2	20.9	53.3	30.8	35.6	43.5	46.5	43.1						34.7

Analyzed in State Geological Analysis Center,Beijing. Major element and La, Ce, Nd, Rb, Ba, Sr, Ni,Zr using ICP-AES; FeO analyzed by titration and K_2O by atomic absorption method, the rest elements by ICP-MS.

in the eclogites of the southern Dulan belt. Garnets have a higher almandine component (45–58 mol%) than those in the SBD, with a correspondingly lower pyrope component (10–27 mol%), and a wider range in the grossular component (13–38 mol%) (Fig. 3A). The omphacite has a similar jadeite component (23–37 mol%) to that in the SBD (Fig. 3B). Calculations based on the present mineral assemblage and composition give $T = 624$–735 °C and $P = 2.0$–2.6 GPa (Yang et al., 2000). However, pseudomorphs of coesite in garnet and exsolution needles of quartz in omphacite indicate that these rocks were metamorphosed under UHP conditions (Song and Yang, 2001). This conclusion is consistent with the discovery of coesite in the gneisses hosting the eclogite blocks (Yang et al., 2001a).

3.5. The eclogite in Altun

The eclogite in Altun consists mainly of garnet + omphacite + rutile + phengite and minor quartz. The omphacite has 32–37 mol% jadeite component (Fig. 3B), whereas the garnet consists of 28–32 mol% pyrope, 41–43 mol% almandine, and 31–32 mol% grossular components (Fig. 3A). The phengite has Si = 6.82–6.96. Polycrystalline quartz occurs as inclusions within large grains of garnet (±2 mm) in eclogite. Some radial fractures are developed around the polycrystalline quartz, and some rectangular polycrystalline quartz inclusions are believed to be coesite pseudomorphs (Zhang et al., 2002). Similar textures have been observed in typical UHP metamorphic belts in the Alps, Norway Caledonides and Dabie-Sulu UHP belt (Carswell and Zhang, 2000). Using the garnet–omphacite–phengite geobarometer and the garnet–omphacite and garnet–phengite geothermometers, two eclogite samples of Altun give $T = 730$ °C, $P = 2.8$ GPa, and $T = 820$–850 °C and $P = 2.9$–3.0 GPa, respectively, conditions typical for the coesite stability field (Zhang et al., 2002).

4. Geochemistry of the eclogite and the Luliangshan volcanic rocks

Thirty-two samples of eclogite and 13 samples of basaltic rocks were analyzed for major and trace elements. Six of the eclogite samples are collected from Altun, seven from Daqaidam, seven from Xitieshan, seven from the northern Dulan belt and five from the southern Dulan belt (Table 1). All 13 igneous samples are collected from Luliangshan and they include eight extrusive rocks, four diabase dikes, and one gabbro (Table 2). All major and trace element measurements were carried out in the National Geological Analysis Center, Beijing, China.

The eclogites in this study are characterized by low LOI contents, most less than 0.5 wt% and average 0.71 wt%, suggesting a hydrous fluid phase was not pervasively present during continental subduction and exhumation. This may also support the statement that the abundances of LIL elements, uranium, and REE patterns in eclogites cannot be easily used to argue for or against chemical mobility, and hence any difference in their concentration could be related to original

Table 2
Chemical compositions of the Luliangshan volcanic rocks, north Qaidam Mountains

Samp Num Rock name	30-12. Lava	30-13. Lava	30-14. Lava	30-20 Lava	30-23 Lava	99Y-418 Lava	99Y-423 Lava	99Y-424 Lava	99Y-414 Diabase	99Y-415 Diabase	30-15. Diabase	30-16. Diabase	99Y-426 Gabbro
SiO2	50.04	49.45	50.3	51.05	51.18	49.80	51.06	50.51	50.73	50.82	49.22	51.02	48.04
TiO2	0.79	1.03	0.98	0.96	1.2	0.98	0.80	0.91	0.64	0.73	1.09	1.18	0.90
Al2O3	13.23	11.36	12.83	13.21	13.19	13.58	13.47	13.77	13.61	13.00	15.11	13.03	19.41
Fe2O3	4.82	3.03	4.4	3.15	3.4	4.07	3.49	3.66	3.48	3.74	5.21	3.52	3.87
FeO	8.32	2.64	10.18	7.89	8.95	10.20	9.25	8.96	8.33	8.81	10.23	9.32	6.00
MnO	0.2	0.1	0.21	0.17	0.24	0.21	0.18	0.17	0.19	0.20	0.21	0.22	0.20
MgO	6.98	7.4	6.21	7.94	6.46	6.67	7.22	7.69	7.92	7.50	5.55	6.43	5.13
CaO	10.6	8.8	9.99	8.32	9.1	8.04	9.32	8.56	10.57	10.01	9.76	9.72	8.93
Na2O	1.36	3.21	1.23	3.53	2.72	3.12	2.14	2.61	2.39	2.58	1.54	1.87	4.15
K_2O	0.14	4.32	0.2	0.05	0.1	0.12	0.18	0.53	0.19	0.22	0.09	0.03	1.06
P2O5	0.08	1.37	0.11	0.1	0.14	0.07	0.06	<0.05	<0.05	0.05	0.11	0.11	0.07
H2O+	2.89	6.73	3.1	3	3.79						2.68	3.13	
LOI	2.14	1.44	2.3	2.66	2.62	1.59	1.57	1.48	1.39	1.53	1.16	2.48	1.23
Total	99.45	99.44	99.74	99.37	100.47	98.45	98.74	98.85	99.44	99.19	100.8	99.58	98.99
[Mg]	0.45	0.73	0.37	0.50	0.41	0.39	0.43	0.46	0.48	0.45	0.35	0.40	0.45
La	2.99	335.8	3.98	3.74	4.78	4.12	3.23	2.31	2.49	3.18	4.09	4.26	18.21
Ce	6.3	560.4	8.6	8.78	10.44	9.94	7.66	6.60	6.07	7.30	8.62	9.66	40.48
Pr	0.94	62.78	1.23	1.4	1.59	1.31	1.00	1.00	0.78	0.94	1.31	1.52	4.85
Nd	4.41	217.6	5.61	6.78	7.28	6.21	4.70	5.13	3.71	4.82	6.2	7.37	20.06
Sm	1.56	36.31	1.92	2.41	2.38	2.23	1.67	2.10	1.25	1.50	2.2	2.61	4.37
Eu	0.61	6.66	0.73	0.74	0.88	0.78	0.57	0.76	0.52	0.61	0.77	0.9	1.31
Gd	1.95	15.98	2.32	2.74	2.75	2.90	2.16	2.75	1.66	2.19	2.7	3.04	4.06
Tb	0.44	1.93	0.5	0.62	0.56	0.57	0.43	0.55	0.38	0.46	0.6	0.66	0.64
Dy	2.65	9.69	2.98	3.8	3.19	4.01	3.12	4.17	2.62	3.02	3.63	4.02	3.70
Ho	0.56	1.85	0.63	0.72	0.65	0.89	0.71	0.92	0.59	0.66	0.75	0.78	0.79
Er	1.63	4.92	1.78	2.16	1.82	2.53	2.00	2.65	1.64	1.80	2.23	2.25	1.94
Tm	0.28	0.32	0.32	0.36	0.31	0.39	0.32	0.41	0.26	0.30	0.38	0.37	0.28
Yb	1.84	1.88	1.95	2.47	1.9	2.71	2.28	2.90	1.86	2.07	2.61	2.38	1.84
Lu	0.29	0.28	0.32	0.37	0.29	0.47	0.40	0.53	0.31	0.36	0.4	0.37	0.31
[La/Ce]N	1.23	1.56	1.20	1.11	1.19	1.08	1.10	0.91	1.07	1.13	1.23	1.15	1.17
[La/Sm]N	1.18	5.70	1.28	0.96	1.24	1.14	1.19	0.68	1.23	1.31	1.15	1.01	2.57
[Sm/Yb]N	1.07	118.13	1.35	1.00	1.66	1.01	0.94	0.53	0.89	1.02	1.04	1.18	6.55
Y	19.96	33.27	25.09	25.36	28.23	28.28	23.34	30.02	19.38	21.77	28.18	27.75	22.63
Sc	34.7	10.78	40.69	31.86	36.08						37.62	32.4	
Rb	8	194	7	3	4	4.1	6.9	16	7.3	5.5	6	2	19
Sr	105	1005	93	98	117	83	172	252	109	136	81	80	1404
Ba	77	1297	54	36	38	55	75	272	62	68	45	23.4	440
Zr	4	283	19	47	46	45	37	44	31	37	21	43	48
Nb	4	23	3	5	5	5.8	3.2	1.6	5.7	3.9	5	5	10
Ta	0.95	0.92	0.35	0.37	0.29	0.5	0.2	0.1	1.0	0.4	0.3	0.33	0.6
U	0.19	12.8	0.27	0.13	0.08	0.4	0.1	0.1	0.3	0.2	0.39	0.21	0.3
Th	0.33	62	0.48	0.34	0.43	0.6	0.3	0.2	1.1	0.4	0.5	0.46	2.8
Hf	2.2	5.6	0.7	0.7	0.79	2.4	1.9	2.2	1.5	1.8	0.54	0.85	2.8
V	224	96	247	192	208	399	364	330	324	332	275	205	237
Cr	75	451	81	63	21	68	92	59	149	73	6	66	15
Ni	83	80	61	68	42	56	62	60	66	62	53	58	12
Co	45	17	46	42	43	43	40	42	37	38	49	46	22

Analyzed in State Geological Analysis Center,Beijing; major element and La, Ce, Nd, Rb, Ba, Sr, Ni,Zr by ICP-AES; FeO by titration and K_2O by atomic absorption method, others by ICP-MS.

differences in the protoliths, and might not be related to gains or losses during metamorphism (Rumble et al., 2003).

In general, eclogites are characterized by low K_2O (average 0.3 wt%) content and low and various SiO_2 content (42–52 wt%), and plot in the basalt field on the silica-alkali diagram (Fig. 4), as well as in the oceanic tholeiitic field on the TiO_2–K_2O–P_2O_5 trident diagram (Holm, 1985). TiO_2 content mainly varies from 0.5–2 wt%, P_2O_5 0.1–0.2 wt%, MgO 5–9 wt% and Al_2O_3 11–15 wt%. Some eclogites have unusual compositions, e.g. two samples from Xitieshan are high in MgO (13–14 wt%); and four samples from the southern Dulan belt have significant higher Al_2O_3 than all the other eclogites. In addition, one sample from the NBD obviously has high TiO_2 (>5 wt%) (Table 1). In diagrams of TiO_2 vs. other oxides and trace elements, the Luliangshan volcanic rocks all plot within the same ranges as the eclogites (Fig. 5). These features suggest that the eclogite protoliths were igneous in origin, but significant differences are obvious from place to place and even in the same locality. According to the TiO_2 contents, the eclogite can be subdivided into three types, high-Ti (TiO_2 = 2–5 wt%), medium-Ti (TiO_2 = 1–2 wt%), and low Ti (TiO_2 < 1 wt%). The geochemical character of the eclogites from different localities and the Luliangshan volcanic rocks are discussed in more detail below.

4.1. Eclogite of Daqaidam

Three of seven analyzed samples (31–34, 31–35a, 32–8) are high-Ti varieties with TiO_2 between 2.4 and 3.4 wt%. Their high K_2O (0.5–1.25 wt%), Na_2O (1.7–3.13 wt%) and P_2O_5 (0.3–0.4 wt%) contents and relatively low SiO_2 (45–46 wt%) and MgO (5–7 wt%) suggest a slightly alkaline tholeiitic composition. These samples are characterized by high total REE abundances and strong LREE enrichment (Fig. 6a), with chondrite-normalized $[La/Yb]_N$ ratios as high as 8.9. MORB-normalized spider diagrams of the high-Ti samples also show strong enrichment in incompatible elements such as K, Rb, Ba, Th, Ta and Nb, and depletion in compatible elements such as Hf, Sc and Cr (Fig. 7a). Such patterns are typical of within-plate basalts (Pearce, 1982). In the Ti/1000 vs. V tectonic discrimination diagram these samples plot in the ocean island basalt (OIB) field (Fig. 8).

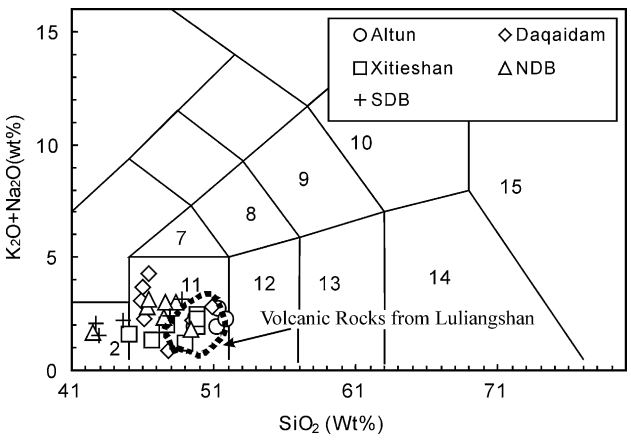

Fig. 4. Na_2O+K_2O vs. SiO_2 diagram showing that the eclogites mainly plot in the basalt and picrite fields, and that the Luliangshan volcanic rocks enclosed by dots plot in the basalt field (after Le Bas et al.,1986).

One sample (32–12) is a medium-Ti type, characterized by low contents of SiO_2 (46 wt%), K_2O (0.02 wt%) and P_2O_5 (0.13 wt%), and slight enrichment in LREE with $[La/Nb]_N$ = 1.8. This sample is similar in composition to the high-Ti type and is classified as ocean island basalt.

The three remaining samples are low-Ti rocks in which TiO_2 ranges from 0.6 to 0.94 wt%. These samples have low K_2O (0.02–0.34 wt%) and P_2O_5 (0.06–0.09 wt%) and are depleted in LREE with $[La/Yb]_N$ 0.2–0.4. In MORB-normalized trace element diagrams, K, Ba, Th, and Nb all show slight depletion, similar features reported from the bask arc type basalts of Mriana Trough and Scotia Sea (Holm, 1985), and plot in the fields of island arc basalt (IAB) and mid-oceanic ridge basalt (MORB) (Fig. 8).

4.2. Xitieshan eclogite

In Xitieshan, both medium- and low-Ti eclogites are present. Five of the seven analyzed samples are medium-Ti in composition with TiO_2 contents between 1.1 and 1.2 wt%. These samples are characterized by moderate SiO_2 (45–50 wt%) and MgO (7.4–9.4 wt%), high Al2O3 (14.7–16.5 wt%) and low K_2O (0.1–0.39 wt%) and P_2O_5 (~0.1 wt%) (Table 1). Chondrite-normalized REE patterns are generally flat, about 10 times chondrite, and show both slight enrichment and slight depletion of LREE (Fig. 6b), with $[La/Nb]_N$ ratios of 1.2–1.4 and 0.8, respectively. These rocks are similar in composition to MORB but are slightly enriched in K, Rb, Th and Ta (Fig. 7b).

Low-Ti eclogites in Xitieshan have very low TiO_2 (0.44–0.54 wt%), high MgO (13–14 wt%), low FeO (7.4) and P_2O_5 (< 0.1 wt%), and high Cr (~1000 ppm) and Ni (~300 ppm). Their chondrite-normalized REE patterns are flat without Eu anomaly and the total REE abundances are five times chondrite with $[La/Nb]_N$ = 0.8–1.2. These samples are similar in many aspects to MORB (Fig. 8B) but are more depleted (Sun et al., 1979), suggesting a gabbro cumulate protolith in an oceanic environment.

4.3. Eclogite in the northern Dulan belt

Eclogites in NBD are medium- and high-Ti types. Five of seven analyzed samples have medium Ti, characterized by TiO_2 between 1.1 and 2.0 wt%, whereas the other two have TiO_2 contents up to 5.48 wt%. The low-Ti samples have moderate SiO_2 (46.3–49.3 wt%), low K_2O (0.1–0.3 wt%) and low P_2O_5 (0.1–0.2 wt%). Most of these rocks are enriched in LREE with $[La/Yb]_N$ = 1.8–3.1, but one sample shows slight LREE's depletion (Fig. 6C). The medium-Ti eclogites have generally flat MORB-normalized trace element patterns (Fig. 7C), but show slight enrichment in Rb, Ba and Th

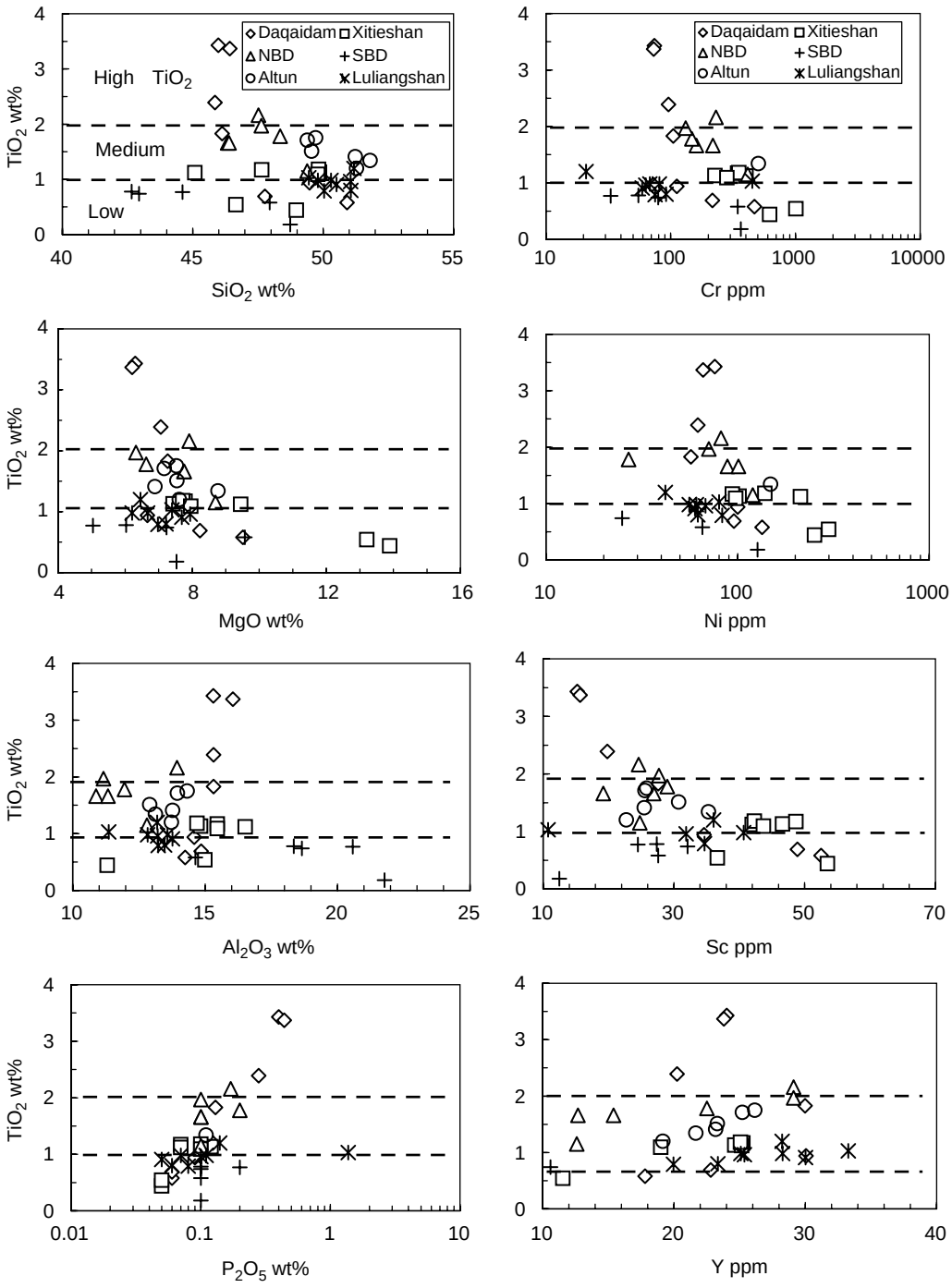

Fig. 5. TiO_2 variation diagrams for the low mobile elements and trace elements of the eclogites and Luliangshan volcanic rocks; eclogites show a wide range in composition with a few high in MgO and Al_2O_3. The Luliangshan volcanic rocks have a similar compositional range as the majority of the eclogites.

and strong enrichment in Cr. Most of these rocks are compositionally similar to MORB but a few show slight depletion in Ta, Nb and Hf, features typical of island arc basalts (Pearce, 1982). Thus, there are probably two protoliths for the medium-Ti eclogites of the northern Dulan belt, MORB and IAT, and compositionally these rocks are similar to low-K basalts formed in a subduction-related environment (Holm, 1985).

High-Ti eclogites in the northern Dulan belt (99Y113, 99Y319) have TiO_2 up to 5.48 wt% (Table 1) but are relatively low in MgO (5.49 wt%), SiO_2 (42.52 wt%), K_2O (0.2–0.49 wt%) and P_2O_5 (0.1–0.17 wt%). LREE's are slightly enriched with $[La/Yb]_N = 6.9$, and the total REE contents are considerably higher (196 ppm) than those in the medium-Ti eclogites (19–80 ppm). These features suggest alkaline oceanic island basalt (Bernard-Griffiths and Cornichet, 1985).

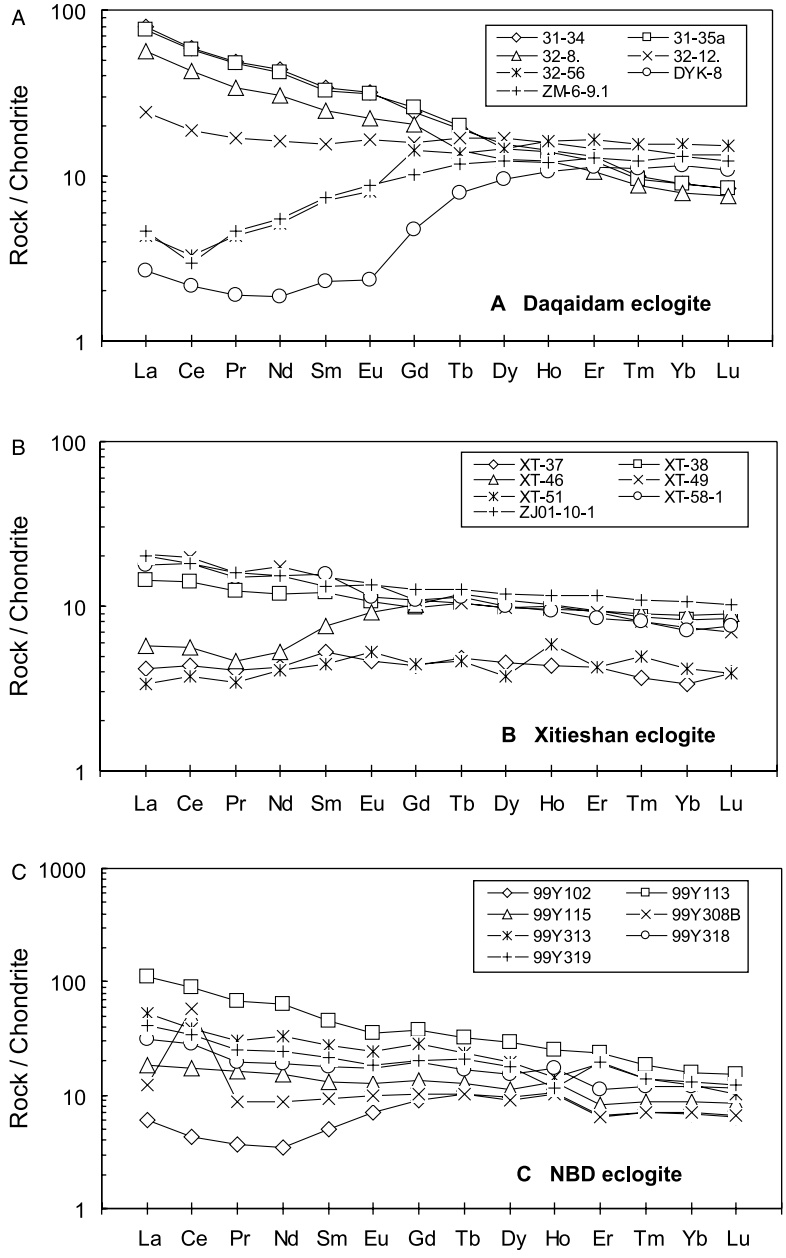

Fig. 6. Chondrite-normalized REE patterns for the eclogites and Luliangshan volcanic rocks.

4.4. Eclogite in the southern Dulan belt

All five analyzed samples in SBD are of the low-Ti variety, characterized by low TiO_2 (0.18–0.78 wt%), K_2O (0.15–0.6 wt%) and P_2O_5 (0.1–0.2 wt%), and high Al_2O_3 (18.4–21.8 wt%), except for one sample with 14.6 wt% Al_2O_3. Total REE show a wide range (9–48 ppm) but all samples have similar chondrite-normalized patterns showing LREE enrichment (Fig. 6D) with $[La/Yb]_N = 3.7–7$. All of the samples also have similar MORB-normalized trace element patterns showing enrichment in Sr, Rb, and Ba, and depletion in Ta, Nb, Zr, Ti, Y, Yb and Cr (Fig. 7D), similar to patterns of island arc tholeiites (Pearce, 1982). Their trace element composition, coupled with their high Al_2O_3 contents suggests that the protoliths were island arc basalts Basaltic Volcanism Study Project (1981).

4.5. The Altun eclogite

The Altun eclogites are medium-Ti varieties but they have relatively higher TiO_2 (1.2–1.7 wt%) and SiO_2 (49.4–51.8 wt%) than other eclogites of this type. The rocks have low K_2O contents (0.01–0.4 wt%), average abundances of MgO 6.9–8.8 and Na_2O 1.8–2.3 wt%, and slightly low Al_2O_3 (13–14 wt%) (Table 1). Total REE abundances of these rocks vary between 30–70 ppm, and both LREE-enriched

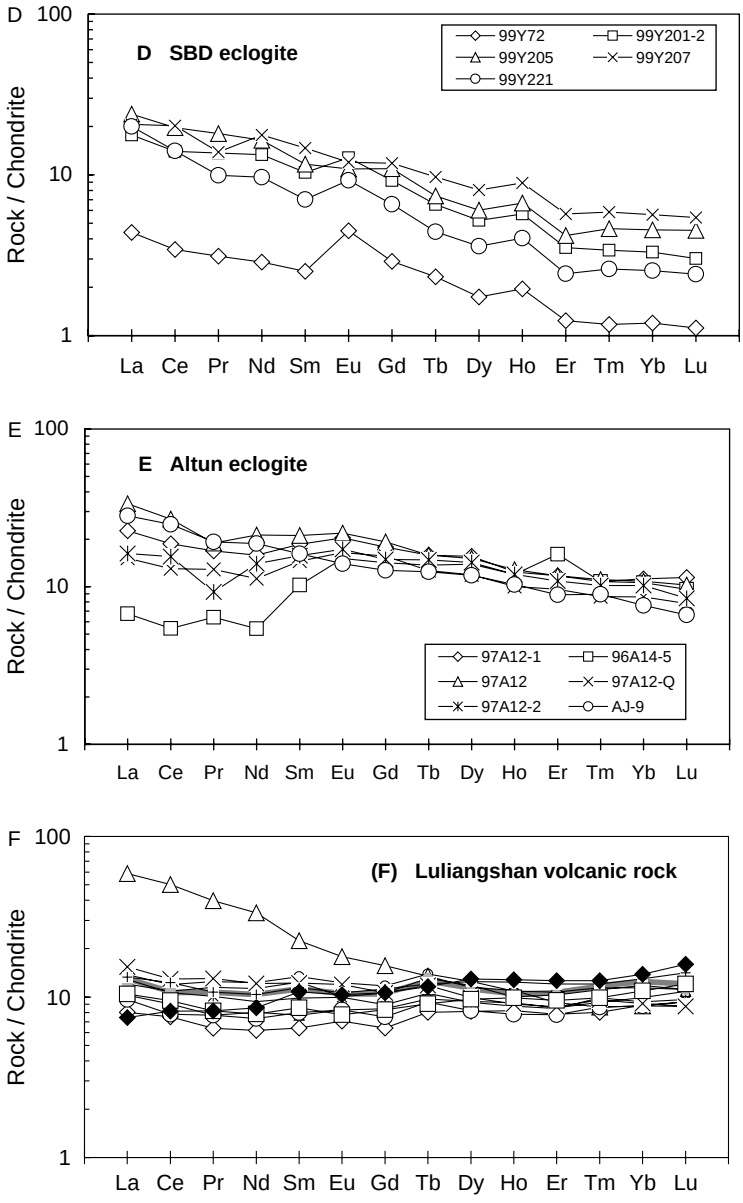

Fig. 6 (*continued*)

and depleted samples are present (Fig. 6E), with $[La/Yb]_N$= 1.6–3.7 and 0.6, respectively. In a MORB-normalized trace element diagram the Altun sample is similar to the eclogites of Xitieshan, i.e. slightly enriched in K, Rb, Ba and Th, and slightly depleted in Y and Yb (Fig. 7E). The major element and trace element data suggest a MORB protolith for these rocks.

4.6. The basaltic sequence of Luliangshan

The Luliangshan basaltic sequence forms a layer a few hundred meters thick in gneisses. Some diabase dikes and gabbros are also present in this sequence and of the 13 samples analyses, eight are lavas, five are diabase dikes and one is gabbro (Table 2).

The lavas and dikes have similar chemical compositions, with TiO_2 ranging from 0.6 to 1.2 wt%, SiO_2 from 49 to 51 wt%, K_2O from 0.15 to 0.6 wt% and P_2O_5 from 0.1 to 0.2 wt%. The compositions are similar to some of the eclogites (Figs. 4 and 5), but no high-Ti basalts found in Lulianshan. The total REE concentrations in these rocks average about 10 times chondrite, and six of seven samples have flat or slightly LREE-depleted chondrite-normalized patterns with $[La/Nb]_N$=0.5–1.6. These compositions are similar to those of typical MORB (Fig. 6f), and in MORB-normalized trace element diagrams the rocks have mainly flat patterns showing slight enrichment in Rb, Ba, Th and Nb. However, some samples show slight depletion in Zr, Hf and Cr, features more characteristic of island arc basalt (Fig. 7f). It is concluded that the Luliangshan basaltic rocks

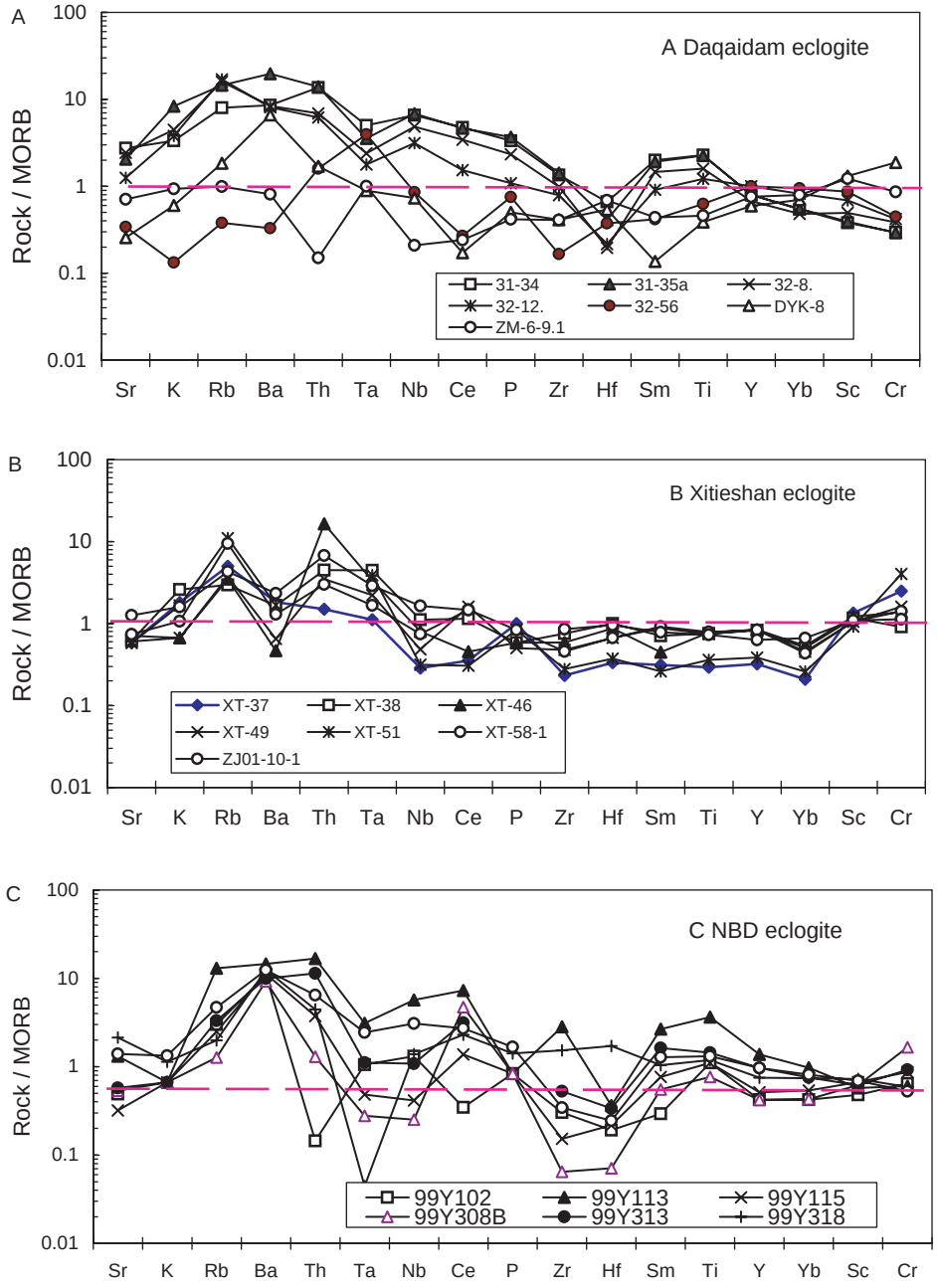

Fig. 7. MORB-normalised multi-elemental plots for eclogites and Luliangshan volcanic rocks.

are mainly MORB but partly island arc basalt, as shown in the Ti/1000 vs. V diagram (Fig. 8). One lava sample, which has high K_2O (4.3 wt%) and P_2O_5 (1.37 wt%), and is strongly enriched in LREE, is considered to be ocean island basalt.

In summary, the basaltic rocks of Luliangshan are compositionally similar to the eclogites of Daqaidam, Xitieshan, NBD and SBD. There are also some greenschist facies metavolcanic rocks in the region with island arc geochemistry, characterized by enrichment in large ion lithophile element (LILE) and LREE (Shi et al., 2004). These rocks are very different from the Luliangshan basaltic rocks and are not considered to be protoliths for any of the eclogites.

4.7. Summary

In general, eclogites in the Altun–north Qaidam UHP terrane have mainly basaltic in compositions and their protoliths, originated in several different tectonic settings, include (1) mid-oceanic ridge basalt, which is the dominant rock type, including low-Ti eclogite in Daqaidam, medium- and low-Ti eclogites in Xitieshan, and medium-Ti eclogite in NBD and Altun, (2) ocean island basalt, including high-Ti eclogite in NBD and both high- and medium-Ti eclogite in Daqaidam, (3) island arc tholeiite, including low-Ti eclogite in SBD. The Luliangshan basaltic rocks, which are compositionally similar to some of the eclogites, formed at mid-ocean spreading ridges and in island arcs.

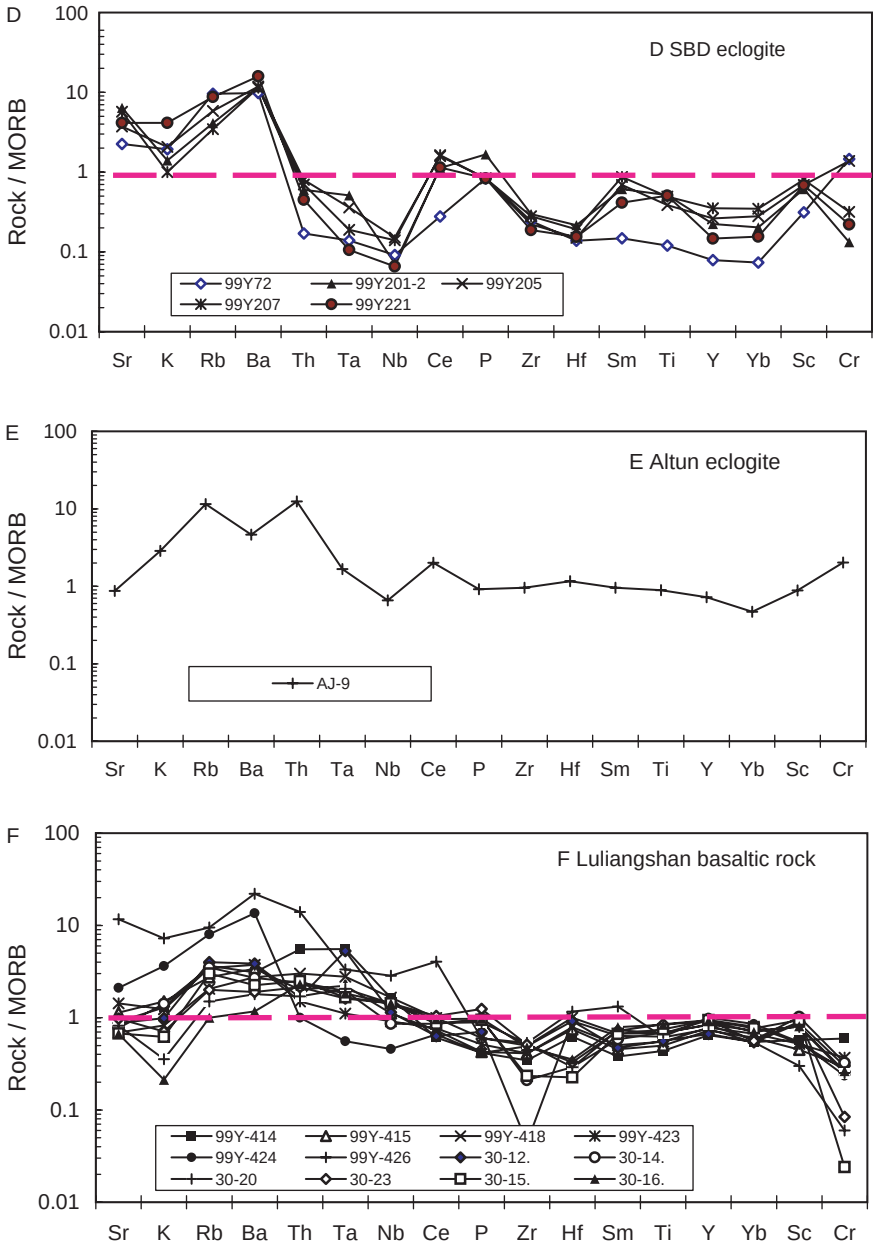

Fig. 7 (*continued*)

5. Nd isotopic compositions of the eclogites and Luliangshan volcanic rocks

Fifteen eclogite samples, including eight from Xitieshan, two from Daqaidam, two from Altun and three from Dulan and six volcanic samples from Luliangshan were analyzed for Sm–Nd isotopes (Table 3). The analyses were carried out at the Isotope Laboratory of the Institute of Geology and Geophysics, Chinese Academy of Science, the Isotope Mass Spectrometer Laboratory of Nanjing University, China and the Sm–Nd Isotope Laboratory of the Department of Earth Sciences, National Cheng Kung University of Taiwan. The analytical procedures followed those of Smith and Huang (1997).

The eight samples from Xitieshan gave εNd(0) of −0.25 to 10.98 and all are positive except sample XT-38 (Fig. 9). U–Pb dating of zircons from the eclogites by TIMS and SHRIMP yielded ages of 485–500 Ma for the eclogite facies metamorphism and ages of 750–800 Ma for the eclogite protoliths (Zhang et al., in press). Thus, the eclogite protoliths yielded εNd(800 Ma) of −0.48 to 9.20, and all samples have positive values except for XT-38. This indicates that the eclogite protoliths were derived from a depleted mantle source. The Nd isotopic signatures of the eclogites are similar to those of MORB, near 0.51325, providing further evidence that the eclogite protoliths were oceanic basalts. Five of the seven analyzed samples have geochemical data, which suggest that the protoliths were

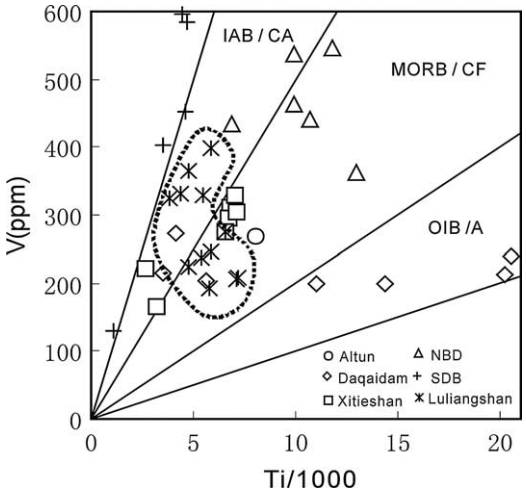

Fig. 8. Ti/1000 vs. V (ppm) diagram (after Shervais, 1982), showing that the eclogite protoliths were basaltic rocks with MORB, IAT and OIB compositions. The Luliangshan basalts are island arc tholeiites and MORB in composition.

low-Ti and medium-Ti basalts. Both the isotopic and geochemical characters of these rocks suggest that the protoliths were MORB probably with a light contamination of crustal material during subduction. Similar isotopic compositions have been reported from eclogites in the Armorican Complex of France and the Cabo Ortegal Complex of Spain, where the protoliths are considered to have formed in an oceanic basin (Bernard-Griffiths and Cornichet, 1985).

All four samples, i.e. two from the Daqaidam and two from the Altun eclogites, show positive εNd(0) values that vary between 0.76–7.85, indicating that the protoliths were derived from a depleted mantle source and suggesting that the rocks formed in an oceanic basin. The geochemistry of the two samples from Altun supports this conclusion, but unfortunately no geochemical data are available for the two Daqaidam samples.

Three eclogite samples from Dulan yielded slightly negative values of εNd(0) ranging from -2.32 to -0.92. The geochemistry of the Dulan eclogites, on the other hand, suggests that the protoliths were MORB, oceanic island basalt and island arc basalt. A reasonable interpretation is that they probably represent oceanic lithosphere that was subducted and slightly contaminated by crustal materials, similar to some eclogite in the Hercynian belt with negative εNd(t) values and interpreted to reflect limited crustal contamination (Kalt et al., 1994).

Thus, both the geochemistry and isotopic character of the eclogites suggest that they were formed by subduction of oceanic crust and that some of them were contaminated by crustal material during subduction. The Sm–Nd isotopic character of the Altun–north Qaidam eclogites is significantly different from that of the eclogites in the Dabie-Sulu UHP terrane, and the latter have large negative εNd(0) values (-10 to -20) (Fig. 9) and are believed to have formed by deep subduction of continental basaltic rocks (Jahn, 1999). The Sm–Nd isotopic signatures of the Altun–north Qaidam eclogites are similar to those of the Variscan orogenic belt in Europe, believed to have been formed by subduction of oceanic crust (Bernard-Griffiths and Cornichet, 1985; Stosch and Lugmair, 1990).

Six analyzed samples of the Luliangshan basaltic rocks have the same Nd isotopic characteristics as the eclogites in the region (Fig. 9). Four of the samples have positive εNd(0) values between 3.02–8.54, and two have slightly negative values of -1.25 to -2.38, suggesting that the amphibole facies metamorphism probably have affected these rocks.

Table 3
Sm–Nd isotope data of eclogite and Luliangshan basaltic rocks from north Qaidam–Altun Mountains

Lacation	Sample No.	Sm(10^{-6})	Nd(10^{-6})	^{147}Sm/^{144}Nd	^{143}Nd/^{144}Nd	$\pm2\sigma$	εNd(0)	εNd(800 Ma)
Xitieshan	QZ19-9	1.004	2.617	0.2319	0.513175	11	10.47	6.88
Xitieshan	XT-37	0.9722	2.745	0.2142	0.513201	17	10.98	9.20
Xitieshan	XT-49	3.3030	11.660	0.1714	0.512767	16	2.52	5.1
Xitieshan	XT-51	0.9898	2.649	0.2260	0.513194	9	10.85	7.86
Xitieshan	XT-33	1.126	2.649	0.2570	0.513110	18	9.21	3.05
Xitieshan	XT-38	2.34	7.11	0.1991	0.512625	9	-0.25	-0.48
Xitieshan	XT-58-1	3.02	9.17	0.1992	0.512762	15	2.42	2.17
Xitieshan	ZJ01-10-1	2.58	9.12	0.1711	0.512714	12	1.48	3.93
Daqaidam	97A25-1	4.550	16.316	0.1687	0.512677	6	0.76	3.62
Daqaidam	QZ16-1	2.666	8.518	0.1893	0.512837	8	3.88	4.64
Altun	97A12-1	4.389	15.777	0.1686	0.512704	9	1.29	4.16
Altun	97A14-5	3.315	9.538	0.2102	0.5134040	14	7.85	6.46
Dulan	Y115	3.158	11.380	0.1679	0.512519	5	-2.32	-1.9
Dulan	Y313	6.041	23.590	0.1549	0.512591	8	-0.92	-0.3
Dulan	Y205	3.033	13.310	0.1379	0.512521	14	-2.28	-1.4
Luliangshan	99y414	1.284	3.405	0.2281	0.512999	10	7.04	3.84
Luliangshan	99y415	1.472	4.696	0.1872	0.512793	11	3.02	3.99
Luliangshan	99y418A	2.372	5.864	0.2409	0.513076	9	8.54	4.03
Luliangshan	99y423	1.598	4.613	0.2177	0.512944	9	5.97	3.83
Luliangshan	99y426	4.291	18.09	0.1435	0.512574	19	-1.25	4.18
Luliangshan	99y427	5.792	25.86	0.1327	0.512516	9	-2.38	4.15

Samples XT-38, XT-58-1, ZJ01-10-1 were analyzed at Cheng Kung University, Tainan, Taiwan; Luliangshan samples were analyzed at the Isotope Mass Spectrometer Laboratory of Nanjing University and the others at the Institute of Geology and Geophysics, Chinese Academy of Science.

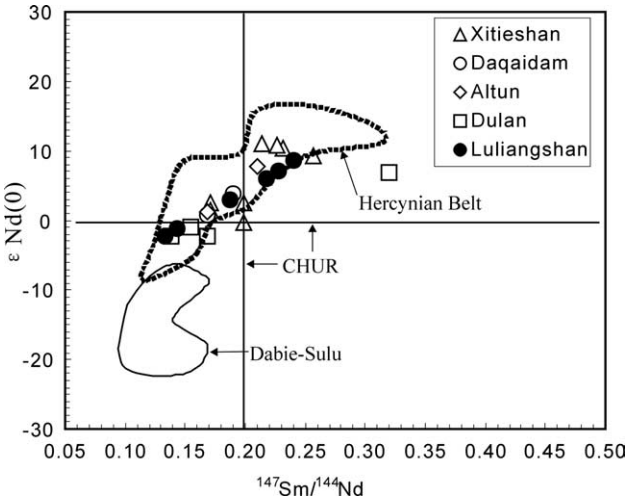

Fig. 9. Nd isotope diagram for the eclogites and Luliangshan volcanic rocks from the north Qaidam and Altun UHPM terranes. High positive and slightly negative values of εNd(0) suggest that the protoliths were oceanic basalts mixed with some continental material during subduction. The Luliangshan volcanic rocks have Nd isotope compositions similar to those of the eclogites. Sm–Nd data for eclogites of the Dabie-Sulu and Variscan orogens (Jahn, 1999), are also shown for comparison.

6. Geochronology of the eclogites and Luliangshan basaltic rocks

6.1. Ages of the eclogites and their protoliths

Various isotopic methods have been used previously to date the eclogites and other UHP metamorphic rocks in the region. Single zircon U–Pb dating by TIMS gave 495±6 Ma for the eclogite of Daqaidam (Zhang et al., 2000) and 504±5 Ma for the eclogite of Altun (Zhang et al., 1999), and both ages were interpreted as the formation age of eclogites. A single zircon from the Xitieshan eclogite dated by the SHRIMP U–Pb technique yielded ages of 485–500 Ma for the rim, which are believed to represent the age of eclogite facies metamorphism, and ages of 750–800 Ma for the core, which are taken as the magmatic crystallization age of the protolith (Zhang et al., 2006).

In this study, two samples of eclogite and one of gneiss were dated by the SHRIMP technique at Stanford University and the data are listed in Table 4. The equipment and methods employed followed those of Barth et al. (2001).

Sample 99Y-115, which is an eclogite from NBD, contains subrounded zircons, 0.1–0.3 mm in length, some of which have prism faces and planes (Fig. 10). Cathodoluminescence (CL) images show that these zircons are homogeneous with no discernable cores. All but one have low Th/U ratios (0.1–0.2) suggesting that the grains formed during metamorphism of the eclogite (Gebauer et al., 1985). Five zircon grains from this sample yielded ages of 443–495 Ma. The Sm–Nd isochron age of the sample gave an age of 457.7±3.3 Ma (Yang et al., 2002b), consistent with the SHRIMP ages.

Sample 99Y-205 is an eclogite from SBD. Six zircon grains from this sample yielded two groups of ages; one with two ages of 487±8.2 and 462±11.6 Ma, and the other with three ages of 968±10.3, 974±13.5 and 1097±14.3 Ma. The first group is believed to represent the age of metamorphism whereas the second group may represent the protolith age of the eclogite. However, because the zircon grains in the second group all have relatively low Th/U ratios (0.04–0.43), they could also represent an early metamorphic age, which is consistent with the protolith age of host gneisses (see next paragraph, sample 99Y-117). One of the six grains, which gave an age of 783±24.8 Ma, has a high Th/U ratio (1.92) suggesting a magmatic origin. This age is similar to the protolith age of the Xitieshan eclogite (750–800 Ma) (Published in this issue).

Sample 99Y-117 is a granitic gneiss from NBD. The zircons from this sample are euhedral, prismatic crystals, and cathodoluminescence images show that the grains have obvious zoning, suggesting a magmatic origin. Most of these zircons have higher abundances of U and radiogenic Pb than

Table 4
SHRIMP U–Pb age data of the zircons seperated from the eclogite and gneiss from Dulan, north Qaidam mountains

Sample	U(ppm)	Th(ppm)	Th/U	±	Pb* (ppm)	204Pb (ppb)	206Pb/ 238U	±	207/235	±	207Pb/ 206Pb	±	238U/ Pb206	±	Pb206/ U238	±
99Y115–1.1	133.8	25.8	0.1926	0.0019	10	9	0.07755	0.00133	0.59	0.0758	0.0552	0.0069	12.895	0.2218	481	8
99Y115–2.1	153.2	16.3	0.1065	0.001	12	5	0.07988	0.00165	0.67247	0.07096	0.06106	0.0062	12.518	0.258	495	9.8
99Y115–3.1	116.1	52.3	0.4507	0.0044	9	7	0.07496	0.00201	0.53705	0.063	0.05196	0.0058	13.341	0.3576	465	12.1
99Y115–4.1	131.9	14.7	0.1112	0.0016	10	9	0.07771	0.00197	0.5914	0.05073	0.0552	0.0044	12.868	0.3263	482	11.8
99Y115–5.1	113.7	11.1	0.098	0.0011	8	6	0.0712	0.00123	0.51956	0.04021	0.0529	0.0039	14.046	0.2425	443	7.4
99Y205–1.1	33.9	65.2	1.9207	0.0325	6	8	0.12926	0.00434	1.2364	0.19814	0.0694	0.0106	7.7361	0.2596	783	24.8
99Y205–2.1	1367.1	56.6	0.0414	0.0002	206	10	0.16212	0.00186	1.5608	0.0254	0.0698	0.0007	6.1682	0.0707	968	10.3
99Y205–3.1	813.8	149.2	0.1834	0.002	148	10	0.18554	0.00263	1.945	0.03665	0.076	0.0008	5.3896	0.0764	1097	14.3
99Y205–4.1	200.2	86.3	0.4312	0.003	34	6	0.16325	0.00244	1.5546	0.04628	0.0691	0.0016	6.1254	0.0914	974	13.5
99Y205–5.1	209.4	9.5	0.0455	0.0005	15	6	0.07853	0.00137	0.59099	0.02639	0.0546	0.0021	12.735	0.2218	487	8.2
99Y205–6.1	125.1	58.6	0.4686	0.0065	10	5	0.07441	0.00194	0.57894	0.05088	0.0564	0.0046	13.438	0.35	462	11.6
99Y117–1.1	513.8	44.9	0.0874	0.001	75	5	0.15566	0.00285	1.5046	0.03788	0.0701	0.0011	6.4241	0.1175	932	15.9
99Y117–2.1	569.7	116	0.2036	0.0018	94	8	0.16968	0.00244	1.7767	0.03678	0.0759	0.001	5.8935	0.0847	1010	13.4
99Y117–2.2	482.8	108.9	0.2256	0.0013	80	41	0.16912	0.00218	1.6576	0.04103	0.0711	0.0014	5.9128	0.0761	1007	12
99Y117–3.1	161	61	0.379	0.0036	27	7	0.16404	0.0029	1.553	0.05216	0.0687	0.0018	6.096	0.1077	979	16.1
99Y117–4.1	545.7	111.2	0.2039	0.0034	90	4	0.16992	0.00291	1.683	0.03602	0.0718	0.0008	5.885	0.1009	1011	16.1

Note: 99Y-115, eclogite, NBD; 99Y-205, eclogite, SBD, 99Y-117, gneiss, NBD.

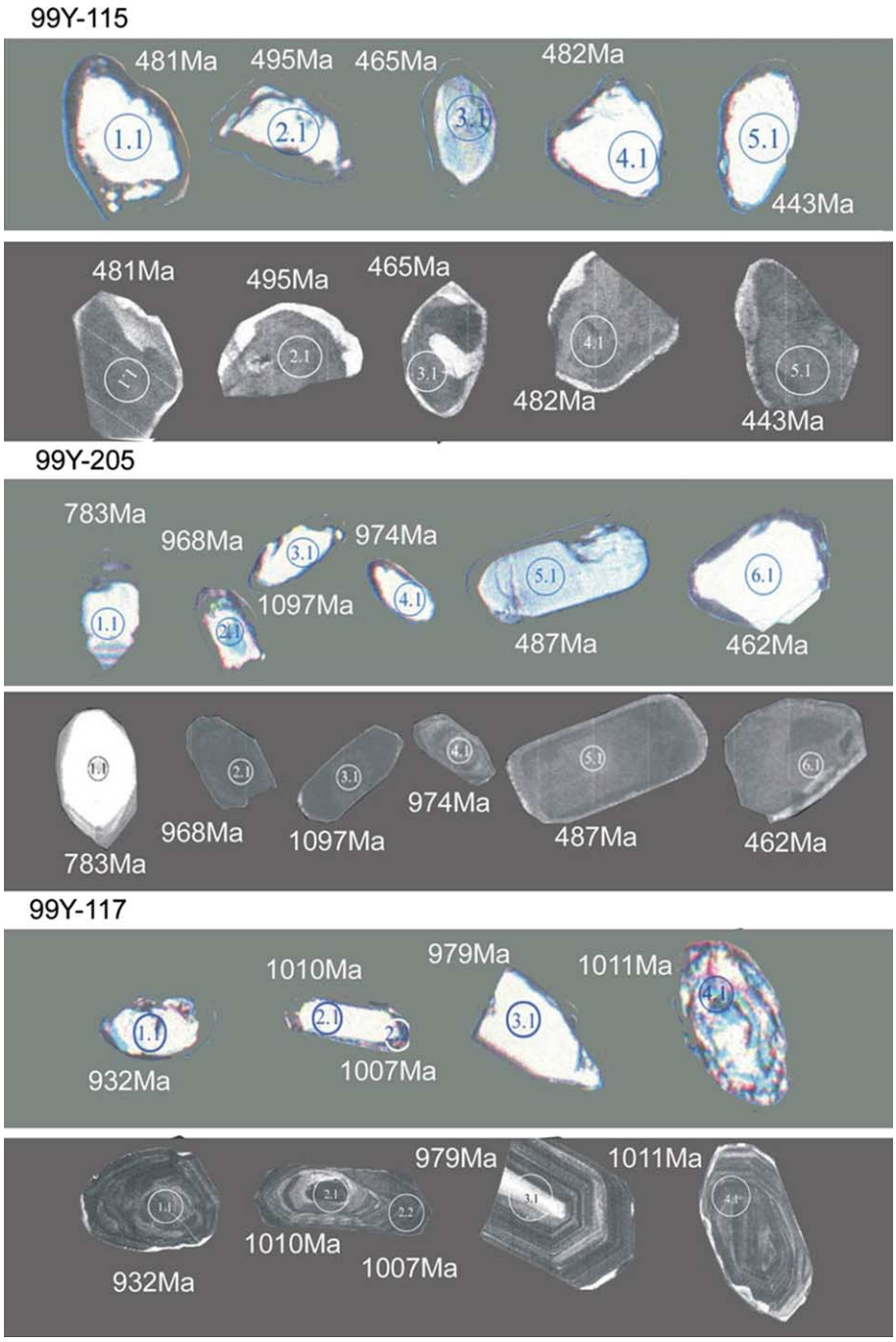

Fig. 10. Cathodoluminescence images of the zircons from the NBD eclogites and gneisses, which are dated by SHRIMP in the present study.

the metamorphic zircons from the eclogite. The four analyzed grains from this sample gave a range of ages between 932 and 1011 Ma, and one grain yielded similar ages for both the rim and core. This suggests that these zircons did not undergo UHP metamorphism in the early Paleozoic. The Th/U ratios of all the zircons from this samples are lower (0.08–0.38) than those of typical magmatic zircons, suggesting a metamorphic protolith for the gneiss (Gebauer et al., 1985).

Based on these data and coupled with SHRIMP ages of 436–497 Ma obtained from garnet peridotite in the north Qaidam UHP metamorphic belt (unpublished data), we suggest that the UHP metamorphism started in early Ordovician, and extended to late Ordovician. Exhumation of the eclogite probably started in Middle Ordovician and continued to the early Silurian. The protoliths of the eclogites have at least two distinct ages, 750–800 and ~1000 Ma. The protolith age of orthogneiss is about 900–1000 Ma, which may reflect another metamorphic event. It should be pointed out that although the gneisses were metamorphosed during subduction, the degree of metamorphism was quite variable. For example, muscovite in the Daqaidam gneiss yielded an Ar–Ar age of 470 Ma, but zircons from the same rock have an age of 1029 Ma (Zhang et al.,

Table 5
Sr–Nd isotope data of the Luliangshan ophiolitic rocks, north Qaidam Mountains

Sample	Rock	Rb(10^{-6})	Sr(10^{-6})	$^{87}Rb/^{86}Sr$	$^{87}Sr/^{86}Sr$	$\pm2\sigma$	Sm(10^{-6})	Nd(10^{-6})	$^{147}Sm/^{144}Nd$	$^{143}Nd/^{144}Nd$	$\pm2\sigma$	$\varepsilon Nd(t)$
99Y414	diabase	7.408	110.90	0.1978	0.707083	25	1.284	3.405	0.2281	0.512999	10	4.0
99Y415	diabase	6.095	141.70	0.2913	0.708092	23	1.472	4.696	0.1872	0.512793	11	4.0
99Y418	lava	3.997	81.85	0.1462	0.706498	21	2.372	5.864	0.2409	0.513076	9	4.2
99Y423	lava	6.735	169.30	0.1187	0.706204	24	1.598	4.613	0.2177	0.512944	9	3.9
99Y426	gabbro	20.13	1397.00	0.0398	0.70534	19	4.291	18.09	0.1435	0.512574	19	4.0
99Y427	clinoyroxenite	53.26	1451.00	0.1046	0.706045	27	5.792	25.86	0.1327	0.512516	9	3.9

Analyses were carried out at the Analysis Center of Mass Spectrometer, Nanjing University.

2000), indicating the zircons have not been reset although the rocks were metamorphosed in the early Paleozoic.

6.2. Ages of the Luliangshan basaltic rocks

We carried out Sr and Nd isotopic analyses on six Luliangshan basaltic rocks, including two tholeiitic lavas, two diabase dikes, one gabbro and one clinopyroxenite (Table 5). Whole-rock sample powders were digested by $HF+HNO_3$ and $HF+HClO_4$. And separation of the Rb, Sr, and the bulk REE was achieved via HCl elution in cation exchange columns. Separation of Sm and Nd was achieved via HCl elution in REE columns. Isotopic analyses for Sr and Nd, as well as isotopic dilution analyses of Rb, Sr, Sm, and Nd were performed at the Isotope Geochemistry Lab, Modern Analysis Center of Nanjing University, China, using a VG354 multiple collector mass spectrometer. The Nd and Sr measurements were corrected for mass fractionation by normalization to $^{146}Nd/^{142}Nd=0.63615$, and $^{86}Sr/^{88}Sr=0.1194$, respectively. Based on comparison with standard values for the NBS987-$SrCO_3$ standard and the La Jolla Nd standard, the precisions ($\pm2\sigma$ uncertainties) for the Sr and Nd isotopic measurements are ±0.000008 and ±0.000006, respectively. The measured $^{87}Sr/^{86}Sr$ for the NBS987 standard is 0.710339 and $^{143}Nd/^{144}Nd$ for the La Jolla Nd standard is 0.511864.

The six analyzed samples show good linear correlations in both the $^{87}Sr/^{86}Sr$ vs. $^{87}Rb/^{86}Sr$, and $^{143}Nd/^{144}Nd$ vs. $^{147}Sm/^{144}Nd$ diagrams. They yield Rb–Sr and Sm–Nd isochronal ages of 768 ± 39 and 780 ± 22 Ma, respectively (Fig. 11). Plots of $^{87}Sr/^{86}Sr$ ratios against Sr concentrations do not define a linear relationship, which also holds for the Sm–Nd system. These observations suggest that the linear correlations do not represent mixing lines. Instead, the Rb–Sr and Sm–Nd isochron ages are interpreted to be the formation age of this suite of rocks. Within the analytical uncertainties, the Rb–Sr isochron age is indistinguishable from the Sm–Nd age.

7. Discussions

The above geochemical data indicate that the protoliths of the eclogite in the Altun–north Qaidam UHPM terrane were MORB, IAT and OIB. The eclogite facies metamorphism took place at 440–500 Ma, whereas the protoliths were formed at 750–800 and ~1000 Ma. The age gap of about 300–500 Ma between UHP metamorphism of eclogites and formation of their protoliths, coupled with the interlayering of eclogite and gneiss, suggest that the protoliths were emplaced into the crust and subducted together with the country rocks. This suggestion is supported by the occurrence of coesite in the gneisses (Yang et al., 2001a). Because the Luliangshan basaltic rocks have compositions and ages similar to those of the eclogites, we

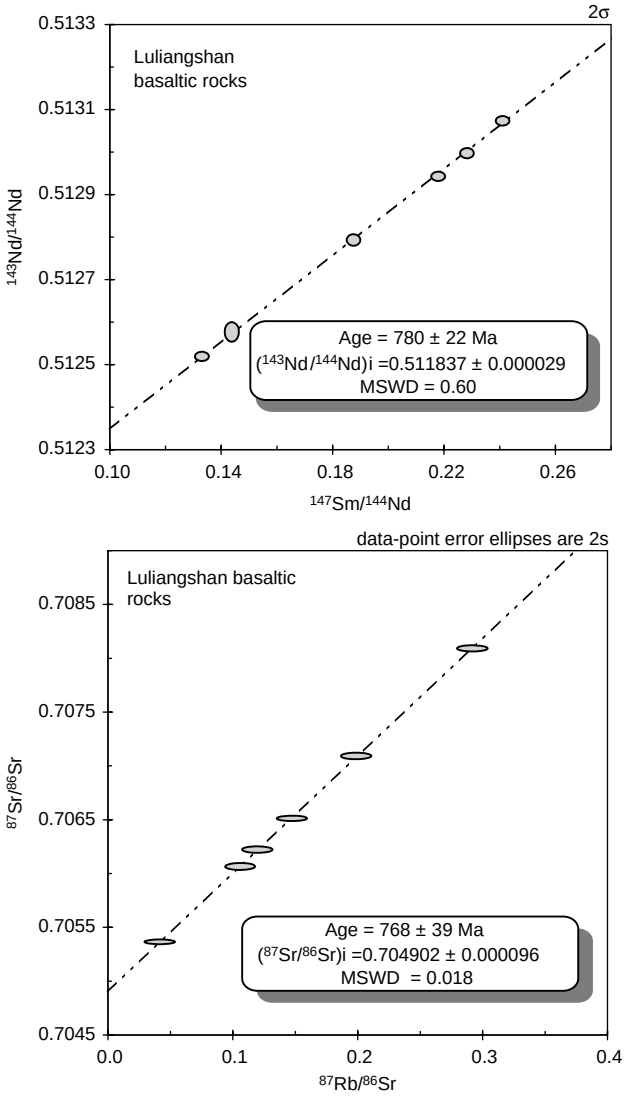

Fig. 11. Sm–Nd and Rb–Sr isochron diagrams for the Luliangshan vocanic rocks.

infer that these bassatic rocks represent Neoproterozoic oceanic crust formed during rifting of Rodinia at 750–800 Ma. These lavas probably were the protoliths for at least some of the eclogites. Subduction-related island arc volcanic rocks and I-type granites of early Paleozoic age in north Qaidam show that an ocean basin closed in the early Paleozoic (Wu et al., 2002; Shi et al., 2004a). The ultrahigh pressure eclogites and crustal gneisses suggest that continental subduction occurred after subduction of the oceanic crust (Yang et al., 2001a; Xu et al., 2003).

The Neoproterozoic protoliths of the eclogite and the presence of oceanic crust of similar age in the Luliangshan region, suggest existence of a Neoproterozoic ocean basin. Several Neoproterozoic ages obtained from the north Qaidam and north Qilian regions support this consideration, e.g. a 729 Ma SHRIMP U–Pb age for zircon grains from granite in Daqaidam (Wu et al., 2004); a 750 Ma U–Pb age for zircon from the K-feldspar granite of Hualong (Wan et al., 2001); a SHRIMP U–Pb age of 760 Ma for cores of the zircon grains from the early Paleozoic Leigongshan tonalitic gneiss (unpublished data); a 780 Ma age for granitic gneiss in Hualong and a 770 Ma age for the Niuxinshan granitic gneiss (Tseng, personal communication). In addition, some reports of Neoproterozoic syn-collisional granites and volcanic rocks in the region can be found in the literature (Lu, 2003; Mao et al., 1998; Wan et al., 2001). All of these observations point to an intense Neoproterozoic magmatism related to the opening and the closing of such oceanic basin in the Qilian region. However, because of the superimposed early Paleozoic tectonic event in the region, most Neoproterozoic rocks have been recycled and can hardly be recognized.

8. Conclusions

Thus, two tectonic events were recognized from the eclogites in the north Qaidan mountains: (1) formation of the Rodinian supercontinent (about 1000 Ma) was followed by formation and destruction of a Neoproterozoic ocean basin (about 750–800 Ma); (2) rifting of the lithosphere formed the Qilian Ocean in the early Paleozoic (>500 Ma), and UHP eclogitic and gneissic rocks formed from previous

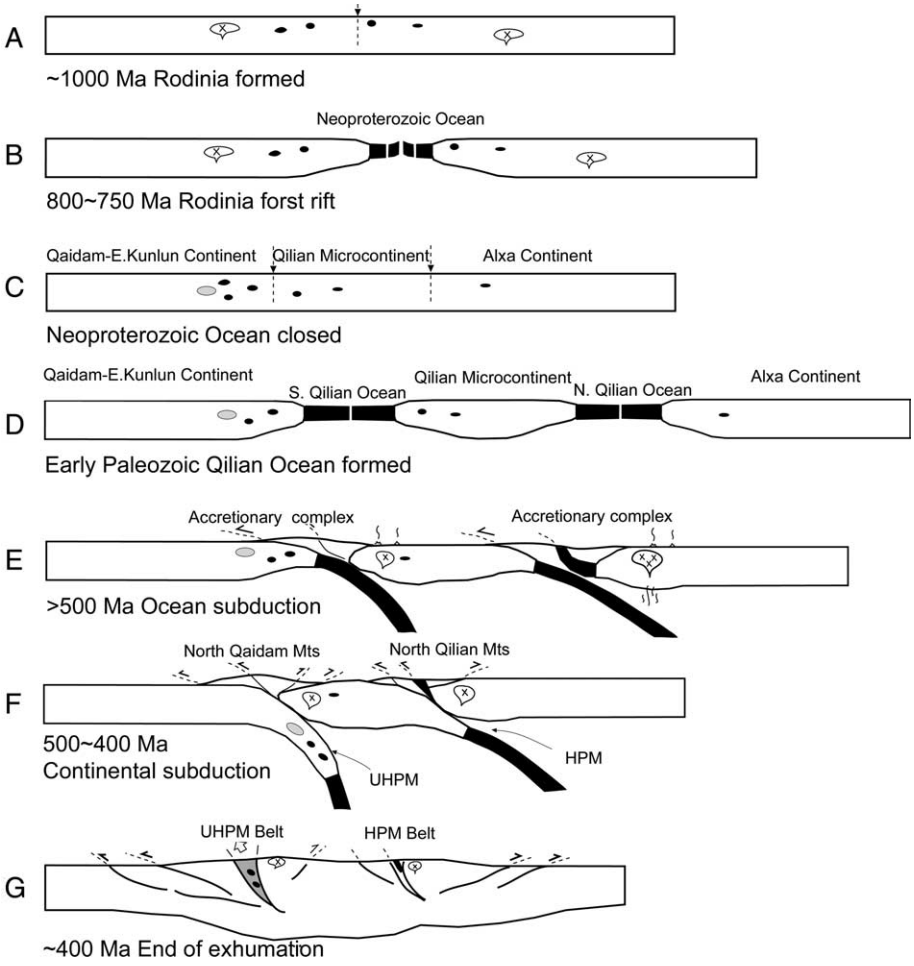

Fig. 12. A cartoon showing two tectonic cycles of ocean basin formation and consumption after formation of Rodinia; one occurred in the Neoproterozoic and the other in the early Paleozoic. (A) The Qilian microcontinent became part of the Rodinian supercontinent at ~1000 Ma; (B,C) rift of Rodinia occurred at about 800–750 Ma, forming an ocean basin; (D,E) after the Neoproterozoic ocean basin closed, the Qilian ocean basin opened and closed in the early Paleozoic; (F,G) UHPM rocks formed after continent–continent collision and deep subduction in north Qaidam and Altun. Protoliths of the eclogite include old oceanic crust formed at ~1000 and 800–750 Ma; Exhumation of UHPM rocks ended at about 400 Ma.

Neoproterozoic oceanic crust and granitic rock during continent–continent collision (500–440 Ma).

Based on the available geochronological and geochemical data, we suggest the following tectonic model for the evolution of the UHP belt in the north Qaidam mountains (Fig. 12). At about 1000 Ma the Qilian area was amalgamated to form the Rodinian continent, which contained some oceanic volcanic rocks, possibly as ophiolitic fragments. This part of Rodinia was then rifted at about 800–750 Ma to form continatal rift valley, which continued to develop into an oceanic basin with mid-ocean ridges and ocean islands. Closure of this ocean basin produced the Neoproterozoic ophiolites and granitic gneisses in the north Qaidam mountains. In the early Paleozoic another Qilian ocean basin formed and subduction of this oceanic lithosphere formed island arc volcanic rocks at about 500 Ma and subduction-related granites at 470–450 Ma. Once the oceanic lithosphere was completely consumed, continent–continent collision followed and led to deep subduction of continental crust, which was tectonically mixed with the eclogites.

Acknowledgements

We thank the Isotope Laboratory of the Institute of Geology and Geophysics, Chinese Academy of Science, the Sm–Nd Isotope Laboratory of the Department of Earth Sciences, National Cheng Kung University of Taiwan, and the Isotope Mass Spectrometer Laboratory of Nanjing University for the Sm–Nd and Rb–Sr isotope analyses. We also thank the National Geological Analysis Center, Beijing, China, for the geochemical analyses and the SHRIMP Laboratory of Stanford University and Secondary Ion Mass Spectrometer (SIMS) in the Research Center of Petrology and Geochemistry, CNRS, Nancy of France, for the U–Pb dating. Special thanks are extended to J.G. Liou for assistance with the laboratory work and Paul Robinson for review of the manuscript. The research was financially supported by MLR (2001CB711001), CGS (200313000058) and NSFC (49732070).

References

Barth, A.P., Wooden, J.L., Coleman, D.S., 2001. SHRIMP-RG U–Pb zircon geochronology of Mesoproterozoic metamorphism and plutonism in the southwesternmost United States. The Journal of Geology 109, 319–327.

Basaltic Volcanism Study Project, 1981. Basaltic Volcanism on the Terrestrial Planets. Pergamon Press, Inc., New York. 1286 pp.

Bernard-Griffiths, J., Cornichet, J., 1985. Origin of eclogites from south Brittany, France: A Sm-Nd isotopic and REE study. Chemical Geology 52 (2), 185–201.

Carswell, D.A., Zhang, R.Y., 2000. Petrographic characteristics and metamorphic evolution of ultrahigh-pressure eclogites in plate-collision belts. In: Ernst, W.G., Liou, J.G. (Eds.), Ultra-High Pressure Metamorphism and Geodynamics in Collision-Type Orogenic Belts. Geological Society of America, pp. 39–56.

Carswell, D.A., O'Brien, P.J., Wilson, R.N., Zhai, M., 1997. Thermobarometry of the phengite-bearing eclogites in the Dabie mountains of the central China. Journal Metamorphic Geology 15 (2), 239–252.

Coleman, R.G., Lee, D.E., Beatty, L.B., Brannock, W.W., 1965. Eclogites and eclogites: their differences and similarities. Bulletin of Geological Society of America 76, 483–580.

Gebauer, D., Lappin, M.A., Grunenfelder, M., 1985. The age and origin of some Norwegian eclogites: a U–Pb zircon and REE study. Chemical Geology 52, 227–248.

Geological Bureau of Qinghai Province, 1991. Geology of Qinghai Province. Geological Publishing House, Beijing.

Holm, P.E., 1985. The geochemical fingerprints of different tectonomagmatic environments using hygramagmatophile element abundances of tholeiitic basalts and basaltic andesites. Chemical Geology 51, 303–323.

Jahn, B.-M., 1999. Sm–Nd isotope tracer of UHP metamorphic rocks: implications for continental subduction and collisional tectonics. International Geology Review 41, 859–885.

Kalt, A., Hanel, M., Schleicher, H., Kranum, U., 1994. Petrology and geochronology of eclogites from the Variscan Schaeavzwald. Contribution to Mineralogy and Petrology 115, 287–302.

Le Bas, M.J., Le Maitre, R.W., Streckeissen, A., Zanettin, B., 1986. A chemical classification of volcanic rocks based on the total alkali-silica diagram. Journal of Petrology 27, 745–750.

Li, H.K., Lu, S.N., Zhao, F.Q., 1999. Geochronology of main Neoproterozoic geological events in the north Qaidam mountains. Geochimica 13 (2), 224–225.

Lu, S.N., 2003. Preliminary Study of Precambrian Geology in the north Tibet–Qinghai Plateau. Geological Publishing House, Beijing p. 125.

Mao, J., Zhang, Z., Yang, J., Song, B., Wu, M., Zuo, G., 1998. Single-zircon dating of Precambrian strata in the west sector of the northern Qilian Mt and its geological significance. Chinese Science Bulletin 43 (15), 1289–1294.

Pearce, J.A., 1982. Trace elements characteristics of lavas from destructive plate boundaries. In: Thorpe, R.S. (Ed.), Andesites. Wiley, Chichesters, pp. 525–548.

Rumble, D., Liou, J.G., Jahn, B.M., 2003. Continental Crust Subduction and Ultrahigh Pressure Metamorphism. Treatise on Geochemistry, vol. 3. Elsevier pp. 293–319.

Shervais, J.W., 1982. Ti–V plots and the petrogenesis of modern and ophiolitic lavas. Earth and Planetary of Science Letters 59, 101–118.

Shi, R.D., Yang, J.S., Wu, C.L., Iizuka, T., Hirata, T., 2004a. Island arc volcanic rocks in the north Qaidam UHP belt, northern Tibet Plateau: evidence for ocean–continent subduction followed by continent–continent subduction. Acta Geologica Sinica 78 (1), 52–63 (in Chinese with English abstract).

Shi, R.D., Yang, J.S., Wu, C.L., Wooden, J.L., 2004b. First SHRIMP dating for the formation of the Late Sinian Yushigou ophiolite, north Qilian mountains. Acta Geologica Sinica 78 (5), 649–658 (in Chinese with English abstract).

Smith, A.D., Huang, L.Y., 1997. The use of extraction chromatographic materials in procedures for the isotopic analysis of neodymium and strontium in rocks by thermal ionization mass spectrometry. Cheng Kung Journal of Science, Engineer & Medicine 32, 1–10.

Song, S.G., Yang, J.S., 2001. Sanidine + quartz inclusions in Dulan eclogites: evidence for UHP metamorphism on the north margin of the Qaidam basin, NW China. Acta Geologica Sinica 75, 180–185 (in Chinese with English abstract).

Sun, S.S., Nesbitt, R.W., Sharaskin, A.Y., 1979. Geochemical characteristics of mid-ocean ridge basalt. Earth and Planetary Science Letters 44, 119–138.

Tsai, C.-O., Liou, J.G., 2000. Eclogite–facies relics and inferred ultrahigh-pressure metamorphism in the north Dabie complex, central–eastern China. American Mineralogist 85, 1–8.

Wan, Y.S., Xu, Z.Q., Yang, J.S., 2001. Ages and compositions of the Precambrian high grade basement of the Qilian terrane and its adjacent areas. Acta Geological Sinica 75 (4), 375–384 (in Chinese with English abstract).

Wu, H., Feng, Y., Song, S., 1993. Metamorphism and deformation of blueschist belts and their tectonic implications, north Qilian Mountains, China. Journal of Metamorphic Geology 11, 523–536.

Wu, C.L., Yang, J.S., Xu, Z.Q., Wooden, J.L., Liou, J.G., Li, H.B., Shi, R.D., Meng, F.C., Persing, H., Meibom, A., 2002. Zircon SHRIMP dating of granite from Qaidamshan, NW China. Chinese Science Bulletin 47 (5), 418–422.

Wu, C.L., Yang, J.S., Xu, Z.Q., Wooden, J.L., Ireland, T., Li, H.B., Shi, R.D., Meng, F.C., Chen, S.Y., Persing, H., Meibom, A., 2004. Granitic magmatism on the early Paleozoic UHP belt of north Qaidam, NW China. Acta Geologica Sinica 78 (3), 658–674.

Xiao, X., Chen, G., Zhu, Z., 1978. The Qilianshan ophiolite and its geological significance. Acta Geologica Sinica 52, 281–295 (in Chinese with English abstract).

Xu, Z.Q., Xu, H.F., Zhang, J.X., 1994. Caledonian subduction and accretion complex. Acta Geologica Sinica 68 (1), 1–15 (in Chinese with English abstract).

Xu, Z.Q., Yang, J.S., Zhang, J.X., 1999. Comparison of the tectonic units on both sides of the Altyn Tagh fault and the mechanism of lithospheric shearing. Acta Geologica Sinica 73, 193–205 (in Chinese with English abstract).

Xu, Z.Q., Yang, J.S., Wu, C.L., Li, H.B., Zhang, J.X., Qi, X.X., Song, S.G., Wan, Y.S., Chen, W., Qiu, H.J., 2003. Timing and machenism of formation and exhumation of the Qaidam ultra-high pressure metamorphic belt. Acta Geologica Sinica 77 (2), 163–176 (in Chinese with English abstract).

Yang, J.S., Xu, Z.Q., Li, H.B., Wu, C.L., Cui, J.W., Zhang, J.X., Chen, W., 1998. Discovery of eclogite at the northern margin of Qaidam basin, NW China. Chinese Science Bulletin 43, 1755–1760.

Yang, J.S., Xu, Z.Q., Song, S.G., Wu, C.L., Shi, R.D., Zhang, J.X., Wan, Y.S., Li, H.B., Jin, X.C., Jalivet, M., 2000a. Discovery of eclogite in Dulan, Qinghai Province and its significance for the HP-UHP metamorphic belt along the central orogenic belt of China. Acta Geologica Sinica 74, 156–168 (in Chinese with English abstract).

Yang, J.S., Xu, Z.Q., Li, H.B., Wu, C.L., Zhang, J.X., Shi, R.D., 2000b. A convergent border at the southern margin of the Qilian terrain, NW China: evidence from eclogite, garnet–peridotite, ophiolite and S-type granite. Journal of the Geological Society of China (Taiwan) 43 (1), 142–160.

Yang, J.S., Xu, Z.Q., Song, S.G., Zhang, J.X., Wu, C.L., Shi, R.D., Li, H.B., Brunel, M., 2001a. Discovery of coesite in the north Qaidam early Paleozoic ultrahigh pressure (UHP) metamorphic belt, NW China. C.R. Acad. Sci. Paris, Sciences de la Terre et des planets/Earth and Planetary Sciences 333, 719–724.

Yang, J.S., Xu, Z.Q., Zhang, J.X., Chu, J.Y., Zhang, R.Y., Liou, J.G., 2001b. Tectonic significance of caledonian high-pressure rocks in the Qilian–Qaidam-Altun mountains, NW China. The Geological Society of American, Memoir 194, 151–170.

Yang, J.S., Xu, Z.Q., Zhang, J.X., Song, S.G., Wu, C.L., Shi, R.D., Li, H.B., Brunel, M., 2002b. Early Palaeozoic north Qaidam UHP metamorphic belt on the north-eastern Tibetan plateau and a paired subduction model. Terra Nova 14, 397–404.

Zhang, J.X., Zhang, Z.M., Xu, Z.Q., Yang, J.S., Cui, J.W., 1999. The ages of U–Pb and Sm–Nd for eclogite from the western segment of Altyn Tagh tectonic belt– the evidences for existence of Caledonian orogenic root. Chinese Science Bulletin 44, 1109–1112 (in Chinese with English abstract).

Zhang, J.X., Yang, J.S., Xu, Z.Q., Zhang, Z.M., Li, H.B., Chen, W., 2000. U–Pb and Ar–Ar ages of eclogites from the northern margin of the Qaidam basin, northwestern China. Journal of the Geological Society of China (Taiwan) 43, 161–169.

Zhang, J.X., Yang, J.S., Xu, Z.Q., Meng, F.C., Li, H.B., Shi, R.D., 2002. Evidence for UHP metamorphism of eclogites from the Altun Mountains. Chinese Science Bulletin 47 (9), 751–755.

Zhang, J.X., Yang, J.S., Meng, F.C., Wan, Y.S., Li, H.M, Wu, C.L., 2006. U–Pb isotopic studies of eclogites and their host gneisses in the Xitieshan area of the north Qaidam Mountains, western China: New evidence for an early Paleozoic HP–UHP metamorphic belt. Journal of Asian Earth Sciences, in press.